Table 2. Upregulated Genes in ALS Motor Neurons (Top 30)

GeneBank No.	Gene Name	Fold Change (ALS/control)
NM_003419	Zinc finger protein 10 (KOX 1)	8.86
U91618	Neurotensin/neuromedin N precursor	8.33*
NM_004651	Ubiquitin-specific protease 11	8.13
D86984	KIAA0231	7.31*
A26792	Ciliary neuronotrophic factor (CNTF)	6.76
M77830	Desmoplakin I & II (DSP; DPI & DPII)	6.10
NM_005622	SA (rat hypertension-associated) homolog	5.47
NM_004733	Acetyl-coenzyme A transporter	5.33
NM_000021	Presenilin 1 (Alzheimer disease 3)	4.96
K03020	Phenylalanine-4-hydroxylase (PAH)	4.95*
AF016268	Death receptor 5 (DR5); cytotoxic TRAIL receptor, TNFR10b	4.91*
M74091	G1/S-specific cyclin C (CCNC)	4.82*
NM_000275	Oculocutaneous albinism II	4.78
AF000936	SH3-binding protein 2	4.73*
NM_000384	Apolipoprotein B	4.70
M63099	Interleukin-1 receptor antagonist	4.66*
M57730	Ephrin-A1	4.57*
L19067	NF-κ B transcription factor p65 subunit	4.52*
U66838	Cyclin A1 (CCNA1)	4.51*
NM_005021	Ectonucleotide pyrophosphatase/phosphodiesterase 3	4.48
NM_001550	Interferon-related developmental regulator 1	4.45
L25851	Integrin alpha E precursor (ITGAE)	4.43*
X16416	C-abl1 protooncogene	4.41
U08015	Transcription factor NF-ATc	4.40*
U44378	Mothers against dpp homolog 4 (SMAD4)	4.35*
NM_005067	Seven in absentia (Drosophila) homolog 2	4.22
J04536	Leukosialin precursor; sialophorin	4.19*
X06745	DNA polymerase alpha catalytic subunit	4.15*
U09564	Serine kinase	4.09*
U37139	β 3-endonexin	4.06*

Gene expression levels are expressed as means of fold-change, which is calculated by dividing the signals of each ALS sample by those of control samples, in the 5 or 10 (denoted by asterisk) patients with ALS.
ALS = amyotrophic lateral sclerosis.

metabolism, and cytoskeletal architecture were downregulated. The functional categories of secreted and extracellular communication proteins and cell cycle regulators were characteristically upregulated. A complete list of the differentially expressed genes is available online at http://www.med.nagoya-u.ac.jp/neurology/index.html.

Differential Gene Expression Profiles between Spinal Motor Neurons and Ventral Horn Homogenates of Amyotrophic Lateral Sclerosis

To compare the expression profile of motor neurons with that of spinal ventral horn homogenates, we performed cluster analyses. Because the patterns of gene expression from microarray analysis are impossible to discern by eye, data analysis software (Acuity 3.0 software; Axon Instruments) was used based on the dimensionality of the data: hierarchical clustering for high dimensional gene space and principal component analysis and SOM for low one. Hierarchical clustering clearly discriminated the expression profile of isolated motor neurons from that of ventral horn homogenates, showing two grouped branches of the dendrogram with a

correlation coefficient of 0.446 (Fig 2A). Moreover, a principal component analysis confirmed the distinction of gene expression profiles between spinal motor neurons and ventral horns (see Fig 2B). The gene expression profile of motor neurons was clustered into a single cluster by the two clustering algorithms, which was well separated from that of spinal ventral horn gray matter, suggesting a relatively uniform degenerating process in spinal motor neurons in ALS.

Motor Neuron–Specific Gene Expression Profiles Identified by the Self-Organizing Map Analysis

To further analyze the expression pattern specific to spinal motor neurons, a SOM was produced as a nonhierarchical clustering.[24,25] The examined genes were subdivided into 25 clustered categories, and the selected genes are shown in a certain group of the SOM (see Fig 2C, Table 6). The genes contained in the clusters reflect the expression pattern in spinal motor neurons as well as that in spinal ventral horns, and these selected genes are somehow different from those in Tables 2 to 5 because of the different bases of classification. Clustering of the SOM showed motor neu-

Table 3. Downregulated Genes in ALS Motor Neurons (Bottom 30)

GeneBank No.	Gene Name	Fold Change (ALS/control)
NM_004378	Cellular retinoic acid–binding protein 1 (CRABP1)	0.12
NM_004430	Early growth response 3 (EGR3)	0.14
NM_005558	Ladinin 1	0.15
NM_003603	Arg/Abl-interacting protein ArgBP2	0.15
NM_000117	Emerin (Emery-Dreifuss muscular dystrophy)	0.15
NM_004357	CD151 antigen	0.15
X06820	Ras homolog gene family member B (RHOB)	0.15*
NM_003834	Regulator of G-protein signalling 11	0.16
NM_002960	S100 calcium-binding protein A3	0.16
NM_006289	Talin	0.16
NM_000964	Retinoic acid receptor, α	0.17
NM_002391	Midkine	0.17
M96944	Paired box protein PAX-5	0.17*
M74178	Hepatocyte growth factor–like protein	0.17*
NM_003822	Nuclear receptor subfamily 5, group A, member 2	0.17
NM_001188	BCL2-antagonist/killer 1; Bak	0.18
NM_000733	CD3E antigen, epsilon polypeptide (TiT3 complex)	0.18
NM_000408	Glycerol-3-phosphate dehydrogenase 2 (mitochondrial)	0.18
NM_000156	Guanidinoacetate N-methyltransferase	0.18*
M11886	Major histocompatibility complex, class I, C	0.18*
NM_003865	Homeo box (expressed in ES cells) 1	0.18
M36340	ADP-ribosylation factor 1 (ARF1)	0.18*
NM_001725	Bactericidal/permeability-increasing protein	0.18
NM_005334	Host cell factor C1 (VP16-accessory protein)	0.19
NM_004192	Acetylserotonin O-methyltransferase–like	0.19
NM_002684	Postmeiotic segregation increased 2–like 11	0.19
M11233	cathepsin D precursor (CTSD)	0.19*
NM_002313	Actin binding LIM protein 1	0.19
NM_002196	Insulinoma-associated 1	0.19
NM_002277	Keratin, hair, acidic, 1	0.19

Gene expression levels are expressed as means of fold-change, which is calculated by dividing the signals of each ALS sample by those of control samples, in the 5 or 10 (denoted by asterisk) patients with ALS.
ALS = amyotrophic lateral sclerosis.

ron–specific upregulated and downregulated gene expression commonly observed in five patients.

Clusters 1 (SOM1) and 6 (SOM6) contains 110 and 169 genes, respectively, that generally are downregulated in spinal motor neurons in all five cases examined, and those are known to be involved in the functional category of cell surface antigens and cell receptors, transcription, and cytoskeleton, whereas clusters 24 (SOM24) and 25 (SOM25) have 191 and 93 genes, respectively, that are predominantly upregulated in spinal motor neurons in all cases and belong to the functional category of cell signaling with extracellular communication, and cell death–associated proteins. The pattern of subcellular localization of their gene products also confirms the characteristics of the functional categories of upregulated and downregulated genes, that is, that plasma membrane and cytoskeletal proteins are more downregulated, and extracellular secreted proteins are more upregulated, in ALS motor neurons. All the genes listed in Table 3 are included in SOM1 and SOM6, whereas SOM24 and SOM25 do not contain all of the genes listed in Table 2. The former group of genes, with downregulation in motor

neurons, included BCL2-antagonist/killer 1 (Bak) and TrkC receptor. Regarding genes related to transcription, early growth response 3 (EGR3), cellular retinoic acid–binding protein 1 (CRABP1), retinoic acid receptors, and Musashi 1 were included in SOM1 and SOM6 as downregulated genes. The expression of dynactin and microtubule-associated proteins (MAPs), which belong to the functional category of cytoskeleton and axonal transport, was downregulated in ALS motor neurons. On the other hand, KIAA0231 and acetyl-coenzyme A transporter were classified into the upregulated genes in motor neurons of ALS. Regarding genes related to cell death, the expression of cyclins A1 and C, death receptor 5 (DR5), and interleukin-1 receptor antagonist was upregulated together with that of NF-κB, tumor necrosis factor (TNF) receptor–associated factor 6 (TRAF6), and caspase-1, -3, and -9 in SOM24 and SOM25. For genes in the category of trophic factor cell signaling with extracellular communication, CNTF, HGF, and glial cell line–derived neurotrophic factor (GDNF) were upregulated in ALS motor neurons, whereas midkine was downregulated. The expression of vascular endothelial growth factor as

Table 4. Upregulated Genes in Spinal Ventral Horns of ALS (Top 30)

GeneBank	Gene Name	Fold Change (ALS/control)
NM_000508	Fibrinogen, A α polypeptide	8.23
D86984	KIAA0231	6.09
NM_001801	Cysteine dioxygenase, type I	5.81
X02544	α-1-Acid glycoprotein 1 precursor	5.59
NM_001973	ELK4, ETS-domain protein (SRF accessory protein 1)	5.12
NM_000021	Presenilin 1 (Alzheimer disease 3)	5.00
NM_002097	General transcription factor IIIA	4.96
U08015	Transcription factor NF-ATc	4.96
M57730	Ephrin-A1	4.88
U91618	Neurotensin/neuromedin N precursor	4.79
AF000936	SH3-binding protein 2	4.50
NM_002949	Mitochondrial ribosomal protein L12	4.11
NM_002386	Melanocortin 1 receptor	4.03
NM_001991	Enhancer of zeste (Drosophila) homolog 1	3.93
NM_000947	Primase, polypeptide 2A (58kDa)	3.92
NM_000239	Lysozyme (renal amyloidosis)	3.88
NM_001550	Interferon-related developmental regulator 1	3.67
NM_004602	Staufen (Drosophila, RNA-binding protein)	3.66
NM_000063	Complement component 2	3.58
NM_004651	Ubiquitin-specific protease 11	3.54
NM_000397	Cytochrome b-245, β polypeptide	3.51
NM_002056	Glutamine-fructose-6-phosphate transaminase 1	3.41
L25851	Integrin α E precursor (ITGAE)	3.36
NM_004616	Transmembrane 4 superfamily member 3	3.21
NM_003720	Down syndrome critical region gene 2	3.18
J04536	leukosialin precursor; sialophorin	3.15
X06745	DNA polymerase alpha catalytic subunit	3.15
K03020	Phenylalanine-4-hydroxylase (PAH)	3.14
NM_001329	C-terminal binding protein 2	3.14
NM_000276	Oculocerebrorenal syndrome of Lowe	3.13

Gene expression levels are expressed as means of fold-change, which is calculated by dividing the signals of each ALS sample by those of control samples, in the five patients with ALS.
ALS = amyotrophic lateral sclerosis.

well as NT-3 was unchanged. Furthermore, the genes whose expression was altered significantly in spinal ventral horn homogenates as shown in Tables 4 and 5 showed similar alterations to some extent in the remaining motor neurons. However, the upregulated genes, such as integrin αE and sialophorin for cell adhesion, which were demonstrated to be spinal ventral horn–derived (see Table 4) as well as spinal motor neuron–derived (Table 2) genes, were not sorted out into SOM24 and SOM25, indicating that their upregulation occurred predominantly in glial cells.

Data Confirmation with Quantitative Real-Time Reverse Transcription Polymerase Chain Reaction, In Situ Hybridization, and Immunohistochemistry

To assure the validity of the gene expression levels detected by microarray analysis, we performed quantitative real-time RT-PCR analysis on some genes of interest using a TaqMan PCR system. Because LCM-isolated motor neurons did not contain enough RNA to perform real-time RT-PCR analysis, only selected genes were assessed in motor neurons, and for other genes the spinal ventral horn homogenates were used as

the template for quantitative RT-PCR. When the extent of increase or decrease of gene expression levels was expressed as the ratio of the genes of interest to GAPDH, acetyl-CoA transporter and KIAA0231 were significantly increased 3.1-fold ($p < 0.001$) and 3.3-fold ($p < 0.01$) in spinal motor neurons of ALS, respectively (Fig 3). EGR3 expression decreased to 0.27-fold ($p < 0.01$) in ALS motor neurons. These mRNA alterations were also detected at comparable levels when using spinal ventral horn homogenates of ALS (acetyl-CoA transporter, 1.8-fold increase [$p < 0.005$]; KIAA0231, 2.3-fold increase [$p < 0.05$]; and EGR3, 0.41-fold decrease [$p < 0.01$]). In addition, the gene expression of Bak and TrkC was downregulated 0.53-fold ($p < 0.01$) and 0.40-fold ($p < 0.05$) in ALS, respectively. Moreover, increases of ephrin A1 and cyclin C expression were observed to the extents of 2.5-fold ($p < 0.05$) and 4.9-fold ($p < 0.01$), whereas dynactin 1 mRNA was downregulated 0.44-fold ($p < 0.01$), and CRABP1 mRNA was also downregulated to 0.59-fold ($p < 0.01$) in ALS.

To further verify the localization and extent of expression of genes of interest, we performed in situ hy-

Table 5. Downregulated Genes in Spinal Ventral Horns of ALS (Bottom 30)

GeneBank	Gene Name	Fold Change (ALS/control)
NM_000843	Glutamate receptor, metabotropic 6	0.22
NM_000730	cholecystokinin A receptor	0.24
NM_003134	Signal recognition particle 14kDa	0.26
NM_003163	Syntaxin 1B	0.27
NM_006476	ATP synthase, H+ transporting, mitochondrial F1F0, subunit g	0.27
NM_001610	Acid phosphatase 2, lysosomal	0.28
NM_003108	SRY (sex determining region Y)-box 11	0.29
NM_001446	Fatty acid binding protein 7, brain	0.30
NM_004583	RAB5C, member RAS oncogene family	0.31
NM_001125	ADP-ribosylarginine hydrolase	0.31
NM_003320	Tubby (mouse) homolog	0.31
NM_001731	B-cell translocation gene 1, antiproliferative	0.31
NM_000999	Ribosomal protein L38	0.32
NM_004128	General transcription factor IIF, polypeptide 2 (30kDa subunit)	0.32
NM_001765	CD1C antigen, c polypeptide	0.32
NM_004430	Early growth response 3 (EGR3)	0.33
K00558	Tubulin, α, ubiquitous	0.33
NM_006732	FBJ murine osteosarcoma viral oncogene homolog B	0.33
NM_002040	GA-binding protein transcription factor, α subunit (60kDa)	0.34
NM_006161	Neurogenin 1	0.35
NM_002684	Postmeiotic segregation increased 2-like 11	0.35
NM_000801	FK506-binding protein 1A (12kDa)	0.35
NM_001051	Somatostatin receptor 3	0.35
NM_005017	Phosphate cytidylyltransferase 1, choline, alpha isoform	0.36
NM_004927	Chromosome 11 open reading frame 4	0.36
NM_000046	Arylsulfatase B	0.37
NM_004378	Cellular retinoic acid–binding protein 1 (CRABP1)	0.37
NM_001998	Fibulin 2	0.38
NM_001839	Calponin 3, acidic	0.38
NM_001183	ATPase, H+ transporting, lysosomal, subunit 1	0.39

Gene expression levels are expressed as means of fold-change, which is calculated by dividing the signals of each ALS sample by those of control samples, in the five patients with ALS.
ALS = amyotrophic lateral sclerosis.

bridization on selected genes. The mRNAs for acetyl-CoA transporter, KIAA0231, and EGR3 were localized in the remaining motor neurons (Fig 4). Spinal motor neurons overexpressed acetyl-CoA transporter and KIAA0231 in ALS, whereas EGR3 was underexpressed. Moreover, TrkC, CRABP1, Bak, and dynactin 1 gene expression was found in motor neurons, and those signals were reduced in ALS. DR5 signals were increased in motor neurons in ALS. Cyclin C signals with punctate immunoreactivity were increased in the cytoplasm as well as in nuclei in ALS motor neurons. The nuclear staining of motor neurons for cyclin C was more prominent in ALS compared with controls.

Discussion

Although reports about differential gene expression using the postmortem spinal cords, including those of patients with ALS, have been published,[26,27] the precise gene expression profiles of the degenerating motor neurons themselves have remained to be elucidated. Laser-captured dissection of motor neurons and subsequent microarray analysis are the most appropriate approaches to understanding the motor neuron–specific

gene expression profile related to the motor neuron degeneration process in sporadic ALS, because these approaches eliminate bias of motor neuron loss, reactive astroglial proliferation, and other cellular reactions. Indeed, serine kinase has been reported to be underexpressed in ALS spinal cord gray matter,[27] but this study showed it was overexpressed in isolated motor neurons, suggesting that the reported underexpression in whole gray matter was influenced by the decreased motor neuron population. In contrast, cathepsin D expression was downregulated in the ALS motor neurons in this study, whereas it was increased in spinal cord gray matter in a previous report,[27] indicating its upregulation in glial cells. In addition, clustering analyses showed that the gene expression profile in the spinal motor neurons was substantially different from that in the whole homogenates of spinal ventral horn gray matter.

The overall microarray analysis using spinal ventral horn homogenates showed gene expression changes in less than 1% of genes examined with more genes showing increased than decreased expression. On the other hand, the motor neuron–specific microarray analysis
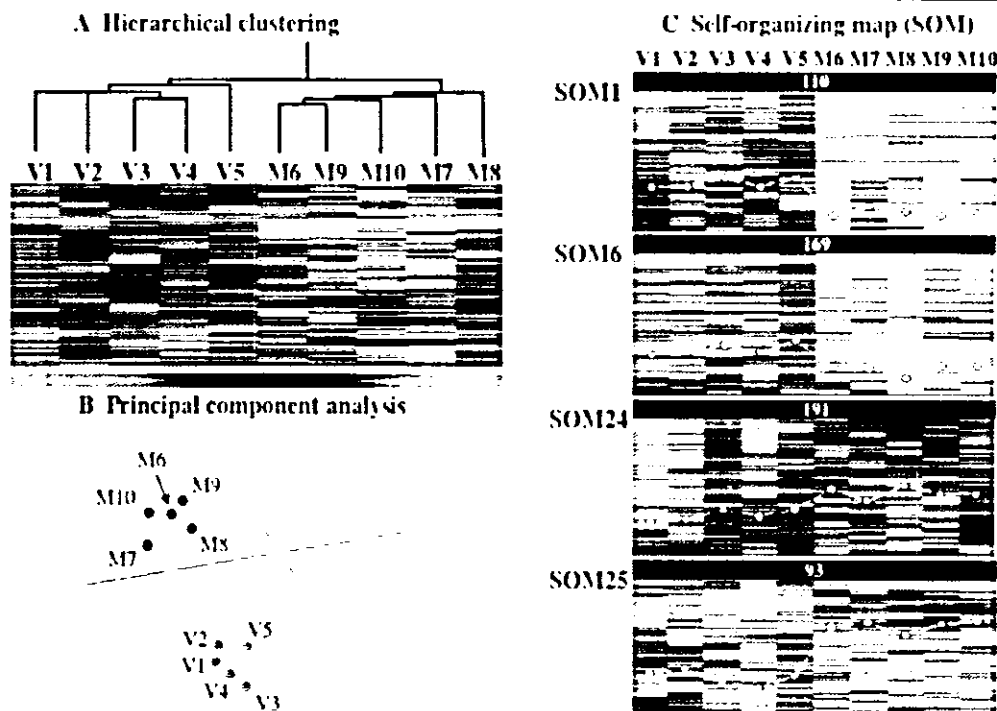
Fig 2. Clustering of gene expression in spinal motor neurons and spinal ventral horns. (A) Hierarchical clustering of gene expression in spinal motor neurons and ventral horns. The dendrogram was produced by hierarchical clustering of relative expression levels of 4,845 genes (rows) in five spinal homogenate and five motor neuron samples (columns) in making a total of 48,450 data points. Visual representation is shown with green representing downregulated (<0.44), black representing intermediate, and red representing upregulated (>2.28). The hierarchical clustering successfully detects two large clusters of amyotrophic lateral sclerosis (ALS), discriminating between spinal homogenates of ventral horns (samples V1 [ALS1], V2 [ALS10], V3 [ALS3], V4 [ALS14], and V5 [ALS13]) and motor neurons (samples M6 [ALS1], M7 [ALS10], M8 [ALS14], M9 [ALS11], and M10 [ALS7]), with a correlation coefficient of 0.446 at the branching point. (B) Principal component analysis of spinal motor neurons and ventral horns. Principal component analysis by six components for the 4,845 genes shows two main clusters consisting of spinal motor neurons (M6–10) and homogenates (V1–5). The number of patients corresponds to those in the dendrogram. (C) Self-organizing map (SOM) analysis of spinal motor neurons and ventral horns. The 4,845 genes are grouped into 25 clusters, the optimal size of which is calculated from gap statistics analysis. In SOM1 and SOM6, most genes are downregulated and in SOM24 and SOM25 the majority of genes are upregulated commonly in isolated motor neurons of five cases (M6–10). The numbers of genes are given at the top, and selected genes are listed for clusters 1, 6, 24, and 25 in Table 6.

showed that the proportion of significantly downregulated genes was 3% of the examined genes, whereas that of upregulated genes was one third of the downregulated genes. Moreover, the genes found to be downregulated specifically in motor neurons were not found to be downregulated in ventral horns, except for three genes with high expression levels. These results strongly support the notion that microarray analysis of laser-captured isolated spinal motor neurons has an advantage especially for the detection of motor neuron–specific downregulated transcripts.

In the differentially expressed genes, cell death–associated genes and genes related to cell signaling were characteristically upregulated in ALS motor neurons, whereas the genes categorized into cytoskeleton and

transcription were downregulated. In the prominently altered genes of interest related to the cell death pathway, acetyl-coenzyme A transporter, which has been cloned and shown to encode a protein with multitransmembranous spanning domains,[28] was overexpressed in ALS motor neurons. Acetyl-CoA transporter functions as a cofactor for acetylation of gangliosides as well as vesicular transport of acetylcholine, which is synthesized from acetyl-CoA and choline. Acetylation has been documented to suppress proapoptotic activity of GD3 ganglioside, which increased in ALS neural tissues, as previously shown.[29,30] These results suggest that enhanced expression of acetyl-CoA transporter may be related to the antiapoptotic mechanism for cholinergic motor neuron degeneration in ALS.

Table 6. Selected Genes Characterized by SOM (select each 15)

GeneBank	Gene Name	Fold Change (ALS/control)
SOM1/6: genes downregulated in ALS motor neurons		
NM_002695	Polymerase (RNA) II (DNA directed) polypeptide E (25kD)	0.20
M24857	Retinoic acid receptor gamma 1 (RAR-γ 1)	0.20
NM_002375	Microtubule-associated protein 4	0.20
NM_001651	Aquaporin 5	0.21
NM_003178	Synapsin II	0.22
NM_004624	Vasoactive intestinal peptide receptor 1	0.23
NM_001740	Calbindin 2, (29kD, calretinin)	0.24
M73812	G1/S-specific cyclin E (CCNE)	0.25
NM_003206	Transcription factor 21	0.25
NM_004082	Dynactin 1 (p150)	0.30
U05012	TRK-C; NT-3 growth factor receptor precursor	0.31
NM_003632	Contactin associated protein 1	0.32
NM_005910	Microtubule-associated protein tau	0.49
NM_002373	Microtubule-associated protein 1A	0.51
NM_002442	Musashi (Drosophila) homolog 1	0.52
SOM24/25: genes upregulated in ALS motor neurons		
M60718	Hepatocyte growth factor (HGF)	3.42
L20814	Glutamate receptor subunit 2 (GLUR-2)	3.34
K02268	β-neoendorphin-dynorphin precursor	3.13
L19063	Glial cell line-derived neurotropic factor (GDNF)	3.08
NM_005543	Insulin-like 3	2.79
J04088	DNA topoisomerase II alpha (TOP2A)	2.58
M22489	Bone morphogenetic protein 2A (BMP2A)	2.57
U51004	Hint protein; protein kinase C inhibitor	2.26
M87507	Caspase 1, interleukin-1 β convertase precursor	2.21
NM_006196	Poly(rC)-binding protein 1	2.16
L29511	Growth factor receptor–bound protein 2	2.04
U78798	TRAF6	1.98
NM_001229	Caspase 9, apoptosis-related cysteine protease	1.89
U84388	Caspase and rip adaptor with death domain (CRADD)	1.83
U13737	Caspase-3	1.77

Gene expression levels are expressed as means of fold-change, which is calculated by dividing the signals of each ALS sample by those of control samples, in the five patients with ALS. Genes listed in Tables 2 and 3 are excluded.
SOM = self-organizing map.

KIAA0231 was one of the mostly overexpressed genes in ALS motor neurons, but the function of this gene product is not known.

In the greatly downregulated genes of interest related to transcription, EGR3, whose expression was remarkably reduced in motor neurons of ALS, is a zinc-finger immediate-early transcription factor that is important for neurotrophin-3 (NT-3) regulation. It is known that EGR3 knockout mice develop gait ataxia, scoliosis, resting tremors, and ptosis due to the degeneration of muscle spindles, through disruption of NT-3 regulation.[31] In ALS motor neurons, TrkC receptor for NT-3 was underexpressed, whereas NT-3 expression was not changed. The finding about TrkC-null mutant and NT-3-null mutant mice show that NT-3-TrkC signaling is required to maintain Ia afferent central synapses of DRG neurons.[32] The marked downregulation of EGR3 in spinal motor neurons may disrupt sensory-motor connections by decreasing NT-3-TrkC signaling, resulting in motor neuron degeneration.

For neurotrophic support for ALS motor neurons, this study showed the overexpression of CNTF, GDNF, and HGF involved in the functional category of cell signaling, suggesting that these neurotrophic factors would be secondarily and compensatorily upregulated after motor neuron degeneration. Indeed, GDNF expression has been reported to increase in the spinal cords and decrease in the muscles of sporadic ALS patients.[33] In contrast with these neurotrophic factors, midkine was one of the significantly downregulated neurotrophic factors. Because midkine plays important roles in promotion of neuronal survival as well as modulation of neuromuscular junctions,[34] its underexpression may be related to motor neuron degeneration. In addition, the gene expression of vascular endothelial growth factor, which has been identified as a critical factor for motor neuron degeneration,[35–37] did not change significantly in gene expression in this study. SOD1 gene expression was not altered in spinal motor neurons and ventral horns. Moreover, the gene expres-
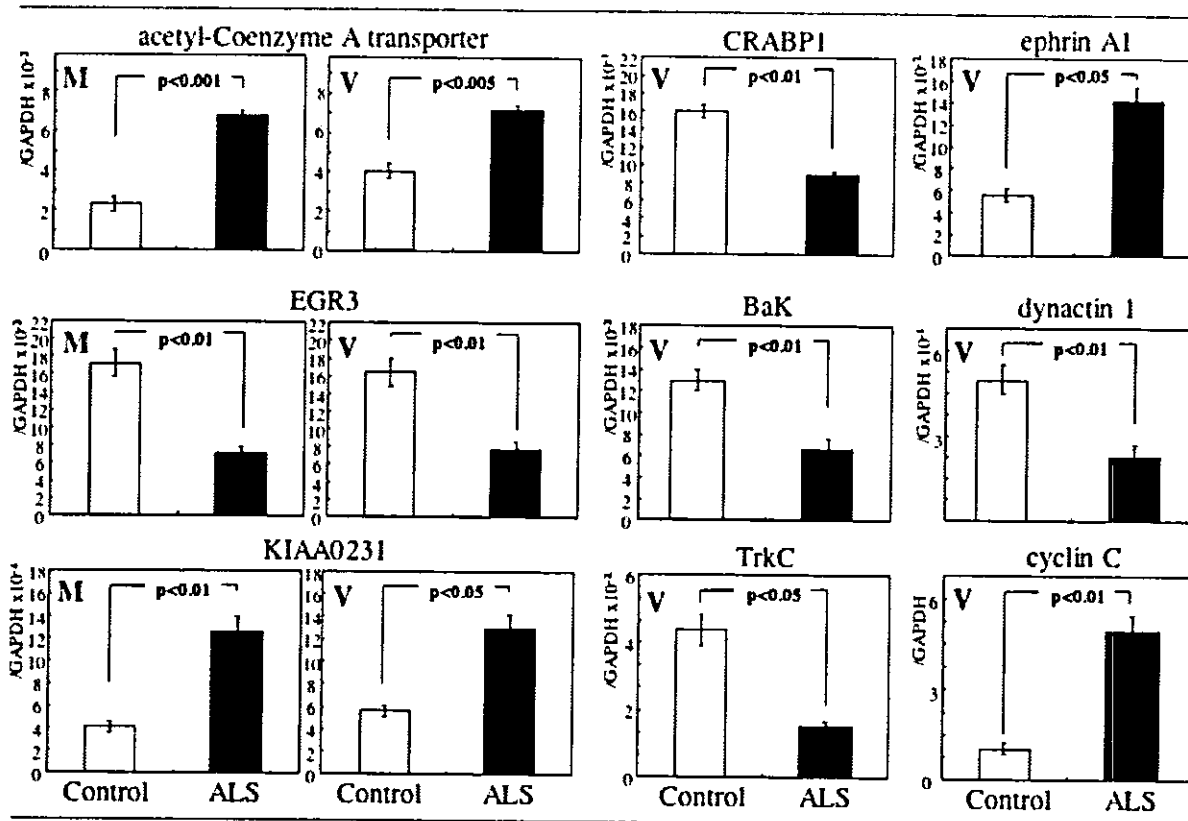
Fig 3. Quantitative real-time reverse transcription polymerase chain reaction verification of the selected genes. Expression levels of acetyl-coenzyme A transporter, EGR3, KIAA0231, CRABP1, Bak, TrkC, ephrin A1, cyclin C, dynactin 1, and GAPDH were measured using spinal motor neurons (M) and ventral horns (V), and those of the target genes were normalized against the GAPDH level. The relative expression levels are expressed as mean ± standard error for 13 amyotrophic lateral sclerosis (ALS) cases and 11 controls. Gene names (Genebank accession number), primers and probe sequences (forward primer, reverse primer, and TaqMan probe; 5' to 3' sequence) were as follows: [acetyl-CoA transporter: D88152] (GGGTTACTTTTTGGGCAATG, AAC-GATTCCTCTGGGTTGAG, FAM-TTGGCCCTTGAATCTGCCGA-TAMRA); [Bak: NM_001188] (CTGGAAGATCAGCAC-CCTAAG, CCCCTCTCCTAGTAGGTCCTG, FAM-TGCTCCCATTCCTCCCTCCG-TAMRA); [CRABP1: NM_004378] (TGCAGGAGTTTAGCCACTTG, CTCACGGGTCCAGTAGGTTT, FAM- TGAGAACAAGATCCACTGCACCCA-TAMRA); [cyclin C: M74091] (TGAGCAGTGGAAGAATTTCG, ACCCTGCTCTCCTTCACTGT, FAM- TGCCAAAACCAAAACCAC-CTCCA-TAMRA); [dynactin 1: NM_004082] (ATGTGAATCGGGAACTGACA, GGGCCTTAGTCTCAGCAAAC, FAM- TG-GAGAGGCAACAGCAGCCAC-TAMRA); [EGR3: NM_004430] (CTTCCCCATGATTCCTGACT, TTGAATGCCTTGATG-GTCTC, FAM-TTCCAGGGCATGGACCCCAT-TAMRA); [ephrin A1: M57730] (GGCAAGGAGTTCAAAGAAGG, TCACCTTCAACCTCAAGCAG, FAM- CCATCCACCAGCATGAAGACCG-TAMRA); [GAPDH: NM_002046] (TCAAGAAG-GTGGTGAAGCAG, GGTGTCGCTGTTGAAGTCAG, FAM-CCTCAAGGGCATCCTGGGCT-TAMRA); [KIAA0231: D86984] (CAACGGTCTTCCAGACAATG, GAGGTTGACCAGCTGTGAGA, FAM-TCCCAGAGGTGAAGCTGCCCTC-TAMRA); and [TrkC: U05012] (TGAGAACCCCCAGTACTTCC, TCAGCACGATGTCTCTCCTC, FAM-CTGCCACAAGCCGGACACGT-TAMRA).

sion level of GluR2 was upregulated, as shown by its classification in SOM25, but the expression of its editing enzyme (adenosine deaminase, RNA-specific, 2; ADAR2) was not altered in this study, although the editing efficiency of GluR2 mRNA has been demonstrated to be low in spinal motor neurons of ALS.[38]

Genes subject to transcriptional regulation constitute a crucial part of the whole human genome as demonstrated by human genome projects.[39] In addition to the gene expression of EGR3, the gene expression of

retinoic acid receptor α and γ together with cellular retinoic acid–binding protein 1 (CRABP1), and Musashi 1, all of which are known to be inducers of neuronal differentiation,[40,41] was downregulated in spinal motor neurons of ALS. The dysregulation of retinoid receptor and retinol binding protein has been reported in the postmortem spinal cords of ALS and SOD1 mutant mice.[17,26] These interesting results imply the potential involvement of the differentiation signals in maintaining motor neuron integrity, which
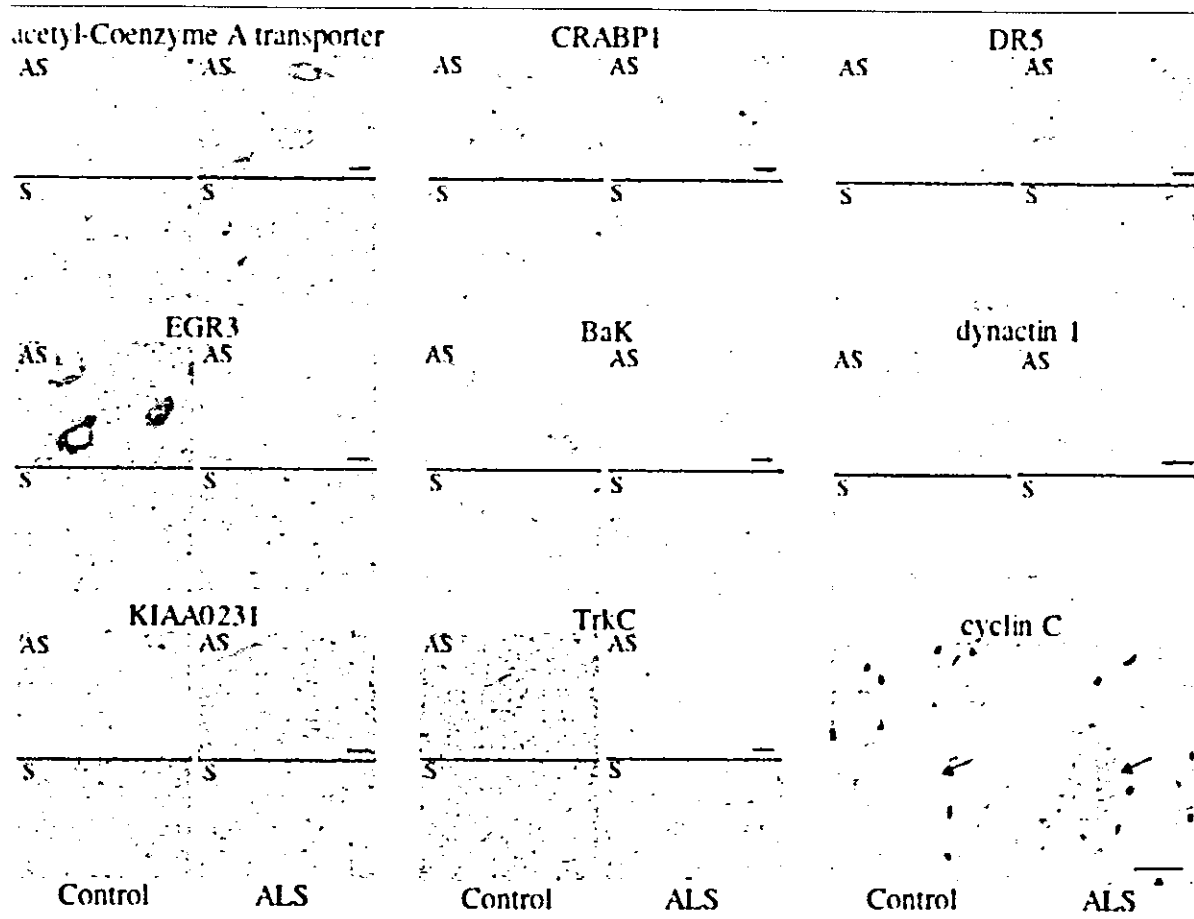
Fig 4. In situ hybridization and immunohistochemistry of the selected genes. Representative in situ hybridization is shown for acetyl-COENZYMEA transporter, EGR3, KIAA0231, CRABP1, Bak, TrkC, DR5, and dynactin 1. The antisense probe (AS) detects positive signals for the expression of each gene in spinal motor neurons for ALS and/or controls, but the sense probe (S) does not. Lipofuscin granules are seen as yellowish granules. Immunohistochemistry was preformed for cyclin C, and nuclear staining was prominent in ALS motor neurons. Arrows denote the nuclei. Bars = 25μm.

might be impaired in the neurodegenerative process of ALS. Among the genes related to transcriptional regulation, the number of significantly downregulated genes was twofold greater than that of the upregulated ones in ALS motor neurons. These downregulated transcription-related genes were not restricted to genes regulating neuronal differentiation as neuron-specific cellular properties, but also included genes such as RNA polymerase and transcription factors, which regulate general cellular functions. These observations suggest that downregulation of transcriptional activity may be the reflection of motor neuron dysfunction because of a wide range of impairments of cellular maintenance systems.

Interestingly, the expression of dynactin 1, which recently has been identified as a causative gene for human motor neuron disease,[42] was reduced in ALS motor neurons. Some other motor proteins including the kinesin family responsible for antegrade axonal trans-

port and dyneins for retrograde axonal transport were not changed significantly, but the expression levels of MAPs 1A, 4, and tau were decreased, shown by their classification in SOM1 and SOM6. The impairment of axonal transport is thought to be an early event of motor neuron degeneration, and especially the protein levels of MAPs 1A and tau have been reported to decrease early before the onset of symptoms in mutant SOD1 transgenic mice.[43–45] The upregulation of ubiquitin-specific protease 11 (USP11), listed in Tables 2 and 3, also may be related to microtubule abnormality because the RanGTP-associated protein RanBPM, which is required for correct nucleation of microtubules, is the enzymatic substrate for USP11.[46] The present results imply that retrograde axonal transport, especially that associated with dynactin, might be affected even at the terminal stage of ALS and be crucial for motor neurons, although cytoskeletal proteins are the major functional group in the downregulated genes.

As for the death signals and inflammatory factors, we previously have reported that these genes were significantly upregulated in the spinal cord of mutant SOD1 transgenic mice,[15,17] suggesting that these inflammatory and apoptotic death signals play a crucial role in concert with motor neuron degeneration and inflammatory cellular reactions, including microglial activation.[7,47] However, in sporadic ALS spinal cords, the expression profiles of inflammation- and death signal–related genes are somewhat different from those in the Tg mouse model. Death receptor 5 (TNF receptor 10b, TNFR10b), TNF receptor–associated factor 6 (TRAF 6), interleukin-1 receptor antagonist, and ephrin A1 were overexpressed in ALS motor neurons, whereas the expression levels of the respective ligands or inducers, TNF-α, TNF superfamily member 10 (TRAIL) and IL-1β, were not markedly changed in either motor neurons or ventral horn homogenates. Because TNF-α was prominently upregulated in the Tg mouse spinal cords,[17] its almost unchanged expression level in sporadic ALS was a surprising observation. Many other inflammation-related genes were also not significantly upregulated in human ALS spinal cords, in contrast with the findings in animal models. Far less invasion and activation of microglia, a major source of TNF-α, IL-1β, and many other inflammatory factors, were seen in human ALS spinal cords at the terminal autopsy stage as compared with those of Tg mice,[48] which could explain these differences.

Genes related to apoptotic pathways, caspase-1, -3, -9, caspase, and RIP adaptor with death domain (CRADD), were upregulated in ALS motor neurons in SOM analysis (SOM24 and SOM25), and an antiapoptotic factor, NF-κB, was markedly upregulated. Although Bax, a proapoptotic Bcl-2 family member, has been reported to increase in ALS motor neurons,[49,50] and another member, Bak, was underexpressed in this study, the expression of Bcl-2 and Bcl-xL, antiapoptotic Bcl-2 family members was not significantly altered in motor neurons, possibly suggesting that Bcl-2 family members are not primarily involved in motor neuron degeneration in sporadic ALS. Cyclin A1 and C were upregulated (SOM25) and cyclin E was downregulated (SOM1) in ALS motor neurons. These cell cycle regulators are specific to G1/S phase transition, and upregulation of these cyclins enhances arrest in G1/S phase, preventing entry into S phase. Our finding on cyclin expression support the recently reported view that G1/S phase is aberrantly activated in ALS motor neurons, eventually inducing motor neuron death.[51] The subcellular localization of cyclin C in the nucleus may trigger cell death signaling mechanisms. These factors related to the cell death signaling pathway, TNFR, TRAF6, CRADD, caspases, cyclins, Bak, and NF-κB may be involved in the motor neuron degeneration process in sporadic ALS, although

we cannot simply state that an apoptotic process is present in ALS motor neurons, as has been suggested by many histological analyses.[6] Becausse neuronal cell degeneration and the eventual neuronal cell death process are the results of interactions of complex pathways involving many factors and signaling molecules, we need to further elucidate the pathophysiological significance of these factors with altered expression levels in ALS motor neurons.

Microarray analysis on the laser-captured motor neurons provided us with significant information about motor neuron degeneration and dysfunction in sporadic ALS patients. Such information cannot be obtained by whole spinal cord tissue microarray assay,[52] as discussed above. Although this study was performed on postmortem patients' tissues, the remaining individual motor neurons would express ongoing or even early molecular events in the neurodegeneration process, because motor neurons in the remaining motor neuron population randomly enter into the degeneration process among up to the terminal stage in ALS.[53] We need to study larger numbers of ALS patients, and to understand the pathophysiological roles of candidate genes identified by the combined methodology of DNA microarray analysis and LCM, compared with other neurodegeneration processes. This methodology provides crucial clues about candidate genes whose related products might hamper the disease process of ALS.

References

1. Ince PG, Lowe J, Shaw PJ. Amyotrophic lateral sclerosis: current issues in classification, pathogenesis and molecular pathology. Neuropathol Appl Neurobiol 1998;24:104–117.
2. Bunina TL. On intracellular inclusions in familial amyotrophic lateral sclerosis. Korsakov J Neuropath Psychiat 1962;62:1293–1296.
3. Okamoto K, Hirai S, Amari M, et al. Bunina bodies in amyotrophic lateral sclerosi immunostained with rabbit anti-cystatin C serum. Neurosci Lett 1993;162:125–128.
4. Cleveland DW, Rothstein JD. From Charcot to Lou Gehrig: deciphering selective motor neuron death in ALS. Nat Rev Neurosci 2001;2:806–819.
5. Bergeron C. Oxidative stress: its role in the pathogenesis of amyotrophic lateral sclerosis. J Neurol Sci 1995;129(suppl):81–84.
6. Sathasivam S, Ince PG, Shaw PJ. Apoptosis in amyotrophic lateral sclerosis: a review of the evidence. Neuropathol Appl Neurobiol 2001;27:257–274.
7. Hand CK, Rouleau GA. Familial amyotrophic lateral sclerosis. Muscle Nerve 2002;25:135–159.
8. Ishigaki S, Liang Y, Yamamoto M, et al. X-Linked inhibitor of apoptosis protein is involved in mutant SOD1-mediated neuronal degeneration. J Neurochem 2002;82:576–584.

9. Kawahara Y, Ito K, Sun H, et al. Glutamate receptors: RNA editing and death of motor neurons. Nature 2004;427:801.

10. Niwa J, Ishigaki S, Hishikawa N, et al. Dorfin ubiquitylates mutant SOD1 and prevents mutant SOD1-mediated neurotoxicity. J Biol Chem 2002;277:36793–36798.

11. Hishikawa N, Niwa J, Doyu M, et al. Dorfin localizes to the ubiquitylated inclusions in Parkinson's disease, dementia with Lewy bodies, multiple system atrophy, and amyotrophic lateral sclerosis. Am J Pathol 2003;163:609–619.

12. Luo J, Isaacs WB, Trent JM, Duggan DJ. Looking beyond morphology: cancer gene expression profiling using DNA microarrays. Cancer Invest 2003;21:937–949.

13. Alizadeh AA, Ross DT, Perou CM, van de Rijn M. Towards a novel classification of human malignancies based on gene expression patterns. J Pathol 2001;195:41–52.

14. Luo L, Salunga RC, Guo H, et al. Gene expression profiles of laser-captured adjacent neuronal subtypes. Nat Med 1999;5: 117–122.

15. Ando Y, Liang Y, Ishigaki S, et al. Caspase-1 and -3 mRNAs are differentially upregulated in motor neurons and glial cells in mutant SOD1 transgenic mouse spinal cord: a study using laser microdissection and real-time RT-PCR. Neurochem Res 2003; 28:839–846.

16. Ginsberg SD, Hemby SE, Lee VM, et al. Expression profile of transcripts in Alzheimer's disease tangle-bearing CA1 neurons. Ann Neurol 2000;48:77–87.

17. Yoshihara T, Ishigaki S, Yamamoto M, et al. Differential expression of inflammation- and apoptosis-related genes in spinal cords of a mutant SOD1 transgenic mouse model of familial amyotrophic lateral sclerosis. J Neurochem 2002;80:158–167.

18. Kamme F, Salunga R, Yu J, et al. Single-cell microarray analysis in hippocampus CA1: demonstration and validation of cellular heterogeneity. J Neurosci 2003;23:3607–3615.

19. Terao S, Sobue G, Hashizume Y, et al. Disease-specific patterns of neuronal loss in the spinal ventral horn in amyotrophic lateral sclerosis, multiple system atrophy and X-linked recessive bulbospinal neuronopathy, with special reference to the loss of small neurons in the intermediate zone. J Neurol 1994;241: 196–203.

20. Sobue G, Hashizume Y, Yasuda T, et al. Phosphorylated high molecular weight neurofilament protein in lower motor neurons in amyotrophic lateral sclerosis and other neurodegenerative diseases involving ventral horn cells. Acta Neuropathol (Berl) 1990;79:402–408.

21. Bohm M, Wieland I, Schutze K, Rubben H. Microbeam MOMeNT: non-contact laser microdissection of membrane-mounted native tissue. Am J Pathol 1997;151:63–67.

22. Watanabe H, Tanaka F, Doyu M, et al. Differential somatic CAG repeat instability in variable brain cell lineage in dentatorubral pallidoluysian atrophy (DRPLA): a laser-captured microdissection (LCM)-based analysis. Hum Genet 2000;107: 452–457.

23. Schutze K, Lahr G. Identification of expressed genes by laser-mediated manipulation of single cells. Nat Biotechnol 1998;16: 737–742.

24. Wang J, Delabie J, Aasheim H, et al. Clustering of the SOM easily reveals distinct gene expression patterns: results of a reanalysis of lymphoma study. BMC Bioinformatics 2002;3: 36–44.

25. Ross ME, Zhou X, Song G, et al. Classification of pediatric acute lymphoblastic leukemia by gene expression profiling. Blood 2003;102:2951–2959.

26. Malaspina A, Kaushik N, de Belleroche J. Differential expression of 14 genes in amyotrophic lateral sclerosis spinal cord detected using gridded cDNA arrays. J Neurochem 2001;77: 132–145.

27. Dangond F, Hwang D, Camelo S, et al. The molecular signature of late-stage human ALS revealed by expression profiling of post-mortem spinal cord gray matter. Physiol Genomics 2004;16:229–239.

28. Kanamori A, Nakayama J, Fukuda MN, et al. Expression cloning and characterization of a cDNA encoding a novel membrane protein required for the formation of O-acetylated ganglioside: a putative acetyl-CoA transporter. Pro Natl Acad Sci USA 1997;94:2897–2902.

29. Malisan F, Franchi L, Tomassini B, et al. Acetylation suppresses the proapoptotic activity of GD3 ganglioside. J Exp Med 2002; 196:1535–1541.

30. Rapport MM, Donnenfeld H, Brunner W, et al. Ganglioside patterns in amyotrophic lateral sclerosis brain regions. Ann Neuol 1985;18:60–67.

31. Chen HH, Tourtellotte WG, Frank E. Muscle spindle-derived neurotrophin 3 regulates synaptic connectivity between muscle sensory and motor neurons. J Neurosci 2002;22:3512–3519.

32. Mears SC, Frank E. Formation of specific monosynaptic connections between muscle spindle afferents and motoneurons in the mouse. J Neurosci 1997;17:3138–3135.

33. Yamamoto M, Sobue G, Yamamoto K, et al. Expression of glial cell line-derived neurotrophic factor mRNA in the spinal cord and muscle in amyotrophic lateral sclerosis. Neurosci Lett 1996; 204:117–120.

34. Zhou H, Muramatsu T, Halfter W, et al. A role of midkine in the development of the neuromuscular junction. Mol Cell Neurosci 1997;10:56–70.

35. Oosthuyse B, Moons L, Storkebaum E, et al. Deletion of the hypoxia-response element in the vascular endothelial growth factor promoter causes motor neuron degeneration. Nat Genet 2001;28:131–138.

36. Lambrechts D, Storkebaum E, Morimoto M, et al. VEGF is a modifier of amyotrophic lateral sclerosis in mice and humans and protects motoneurons against ischemic death. Nat Genet 2003;34:383–394.

37. Gros-Louis F, Laurent S, Lopes AA, et al. Absence of mutations in the hypoxia response element of VEGF in ALS. Muscle Nerve 2003;28:774–775.

38. Kawahara Y, Ito K, Sun H, et al. Low editing efficiency of GluR2 mRNA is associated with a low relative abundance of ADAR2 mRNA in white matter of normal human brain. Eur J Neurosci 2003;18:23–33.

39. Venter JC, Adams MD, Myers EW, et al. The sequence of the human genome. Science 2001;291:1304–1351.

40. Colbert MC, Rubin WW, Linney E, LaMantia AS. Retinoid signaling and the generation of cellular diversity in the embryonic mouse spinal cord. Dev Dyn 1995;204:1–12.

41. Sakakibara S, Okano H. Expression of neural RNA-binding proteins in the postnatal CNS: implications of their roles in neuronal and glial cell development. J Neurosci 1997;17: 8300–8312.

42. Puls I, Jonnakuty C, LaMonte BH, et al. Mutant dynactin in motor neuron disease. Nat Genet 2003;33:455–456.

43. Williamson TL, Cleveland DW. Slowing of axonal transport is a very early event in the toxicity of ALS-linked SOD1 mutants to motor neurons. Nat Neurosci 1999;2:50–56.

44. Zhang B, Tu P, Abtahian F, et al. Neurofilaments and orthograde transport are reduced in ventral root axons of transgenic mice that express human SOD1 with a G93A mutation. J Cell Biol 1997;139:1307–1315.

45. Farah CA, Nguyen MD, Julien JP, Leclerc N. Altered levels and distribution of microtubule-associated protein before disease onset in a mouse model of amyotrophic lateral sclerosis. J Neurochem 2003;84:77–86.

46. Ideguchi H, Ueda A, Tanaka M, et al. Structural and functional characterization of the USP11 deubiquitinating enzyme, which interacts with the RanGTP-associated protein RanBPM. Biochem J 2002;367:87-95.

47. Hensley K, Floyd RA, Gordon B, et al. Temporal patterns of cytokines and apoptosis-related gene expression in spinal cords of the G93A-SOD1 mouse model of amyotrophic lateral sclerosis. J Neurochem 2002;82:365-374.

48. Hall ED, Oostveen JA, Gurney ME. Relationship of microglial and astrocytic activation to disease onset and progression in a transgenic model of familial ALS. Glia 1998;23:249-256.

49. Mu X, He J, Anderson DW, et al. Altered expression of bcl-2 and bax mRNA in amyotrophic lateral sclerosis spinal cord motor neurons. Ann Neurol 1996;40:379-386.

50. Ekegren T, Grundstrom E, Lindholm D, Aquilonius SM. Up-regulation of Bax protein and increased DNA degradation in ALS spinal cord motor neurons. Acta Neurol Scand 1999;100:317-321.

51. Ranganathan S, Bowser R. Alterations in G(1) to S phase cell-cycle regulators during amyotrophic lateral sclerosis. Am J Pathol 2003;162:823-835.

52. Malaspina A, de Belleroche J. Spinal cord molecular profiling provides a better understanding of amyotrophic lateral sclerosis pathogenesis. Brain Res Brain Res Rev 2004;45:213-229.

53. Sobue G, Sahashi K, Takahashi A, et al. Degenerating compartment and functioning compartment of motor neurons in ALS: possible process of motor neuron loss. Neurology 1983;33:654-657.

Physical and Functional Interaction between Dorfin and Valosin-containing Protein That Are Colocalized in Ubiquitylated Inclusions in Neurodegenerative Disorders*

Shinsuke Ishigaki‡§¶, Nozomi Hishikawa‡, Jun-ichi Niwa‡, Shun-ichiro Iemura‖, Tohru Natsume‖, Seiji Hori**, Akira Kakizuka**‡‡, Keiji Tanaka§, and Gen Sobue‡§§

From the ‡Department of Neurology, Nagoya University Graduate School of Medicine, Nagoya 466-8500, Japan, the §Department of Molecular Oncology, Tokyo Metropolitan Institute of Medical Science, Tokyo 113-8613, Japan, the ‖National Institute of Advanced Science and Technology, Biological Information Research Center, Tokyo 135-0064, Japan, the **Laboratory of Functional Biology, Kyoto University Graduate School of Biostudies, Kyoto 606-8502, Japan, and ‡‡CREST, Japan Science and Technology Agency, Kawaguchi 332-0012, Japan

Dorfin, a RING-IBR type ubiquitin ligase (E3), can ubiquitylate mutant superoxide dismutase 1, the causative gene of familial amyotrophic lateral sclerosis (ALS). Dorfin is located in ubiquitylated inclusions (UBIs) in various neurodegenerative disorders, such as ALS and Parkinson's disease (PD). Here we report that Valosin-containing protein (VCP) directly binds to Dorfin and that VCP ATPase activity profoundly contributes to the E3 activity of Dorfin. High through-put analysis using mass spectrometry identified VCP as a candidate of Dorfin-associated protein. Glycerol gradient centrifugation analysis showed that endogenous Dorfin consisted of a 400–600-kDa complex and was co-immunoprecipitated with endogenous VCP. In vitro experiments showed that Dorfin interacted directly with VCP through its C-terminal region. These two proteins were colocalized in aggresomes in HEK293 cells and UBIs in the affected neurons of ALS and PD. VCP^{K524A}, a dominant negative form of VCP, reduced the E3 activity of Dorfin against mutant superoxide dismutase 1, whereas it had no effect on the autoubiquitylation of Parkin. Our results indicate that VCPs functionally regulate Dorfin through direct interaction and that their functional interplay may be related to the process of UBI formation in neurodegenerative disorders, such as ALS or PD.

Amyotrophic lateral sclerosis (ALS)[1] is one of the most common neurodegenerative disorders, characterized by selective

[1] The abbreviations used are: ALS, amyotrophic lateral sclerosis; E3, ubiquitin ligase; ERAD, endoplasmic reticulum-associated degradation; LB, Lewy body; MS, mass spectrometry; LC-MS/MS, liquid chromatography coupled to electrospray tandem mass spectrometry; PD, Parkinson's disease; SOD1, CuZn-superoxide dismutase; UBI, ubiquitylated inclusions; VCP, valosin-containing protein; FLAG-Parkin, pcDNA3.1/FLAG-Parkin; Ub, ubiquitin; MBP, maltose-binding protein; GST, glutathione S-transferase; PBS, phosphate-buffered saline; HA, hemagglutinin; WT, wild type.

motor neuron degeneration in the spinal cord, brain stem, and cortex. Two genes, CuZn-superoxide dismutase (SOD1) and amyotrophic lateral sclerosis 2 have been identified as responsible genes for familial forms of ALS. Using mutant SOD1 transgenic mice, the pathogenesis of ALS has been partially uncovered. The proposed mechanisms of the motor neuron degeneration in ALS include oxidative toxicity, glutamate receptor abnormality, ubiquitin proteasome dysfunction, inflammatory and cytokine activation, dysfunction of neurotrophic factors, damage to mitochondria, cytoskeletal abnormalities, and activation of the apoptosis pathway (1, 2).

In a previous study (3), we identified several ALS-associated genes using molecular indexing. Dorfin was identified as one of the up-regulated genes in ALS, which contains a RING-IBR (in between ring finger) domain at its N terminus and mediated ubiquitin ligase (E3) activity (3, 4). Dorfin colocalized with Vimentin at the centrosome after treatment with a proteasome inhibitor in cultured cells (4). Dorfin physically bound and ubiquitylated various SOD1 mutants derived from familial ALS patients and enhanced their degradation, but it had no effect on the stability of wild-type SOD1 (5). Overexpression of Dorfin protected neural cells against the toxic effects of mutant SOD1 and reduced SOD1 inclusions (5).

Recent findings indicate that the ubiquitin-proteasome system is widely involved in the pathogenesis of Parkinson's disease (PD), Alzheimer's disease, polyglutamine disease, and Prion diseases as well as ALS (6). From this point of view, we previously analyzed the pathological features of Dorfin in various neurodegenerative diseases and found that Dorfin was predominantly localized not only in Lewy body (LB)-like inclusions in ALS but also in LBs in PD, dementia with Lewy bodies, and glial cell inclusions in multiple system atrophy (7). These characteristic intracellular inclusions composed of aggregated, ubiquitylated proteins surrounded by disorganized filaments are the histopathological hallmark of aging-related neurodegenerative diseases (8).

A structure called aggresome by Johnston et al. (9) is formed when the cell capacity to degrade misfolded proteins is exceeded. The aggresome has been defined as a pericentriolar, membrane-free, cytoplasmic inclusion containing misfolded ubiquitylated protein ensheathed in a cage of intermediate filaments, such as Vimentin (9). The formation of the aggresome mimics that of ubiquitylated inclusions (UBIs) in the affected neurons of various neurodegenerative diseases (10). Combined with the fact that Dorfin was localized in aggresomes in cultured cells and UBIs in ALS and other neurode-

generative diseases, these observations suggest that Dorfin may have a significant role in the quality control system in the cell. The present study was designed to obtain further clues for the pathophysiological roles of Dorfin. For this purpose, we screened Dorfin-associated proteins using high performance liquid chromatography coupled to electrospray tandem mass spectrometry (LC-MS/MS). The results showed that Valosin-containing protein (VCP), also called p97 or Cdc48 homologue, obtained from the screening, physically and functionally interacted with Dorfin. Furthermore, both Dorfin and VCP proteins colocalized in aggresomes of the cultured cells and in UBIs in various neurodegenerative diseases.

MATERIALS AND METHODS

Plasmids and Antibodies—pCMV2/FLAG-Dorfin vector (FLAG-Dorfin^{WT}) was prepared by PCR using the appropriate design of PCR primers with restriction sites (ClaI and KpnI). The PCR product was digested and inserted into the ClaI-KpnI site in pCMV2 vector (Sigma). pEGFP-Dorfin (GFP-Dorfin), pCMX-VCP^{Wt} (VCP^{Wt}), and pCMX-VCP^{K524A} (VCP^{K524A}) vectors were described previously (5, 11). pcDNA/HA-VCP^{Wt} (HA-VCP^{Wt}) and pcDNA/HA-VCP^{K524A} (HA-VCP^{K524A}) were subcloned from pCMX-VCP^{Wt} and pCMX-VCP^{K524A}, respectively, into pcDNA3.1 vectors (Invitrogen). The HA tag was introduced at the N terminus of VCP. pcDNA3.1/FLAG-Parkin (FLAG-Parkin) was generated by PCR using the appropriate design of PCR primers with restriction sites (EcoRI and NotI) from pcDNA3.1/Myc-Parkin (12). The FLAG tag was introduced at the N terminus of Parkin. To establish the RING mutant plasmid of Dorfin (FLAG-Dorfin$^{C132S/C135S}$), point mutations for Cys at positions 132 and 135 to Ser were generated by PCR-based site-directed mutagenesis using a QuikChange™ site-directed mutagenesis kit (Stratagene, La Jolla, CA). pcDNA3.1/HA-Ub (HA-Ub), pcDNA3.1/Myc-SOD1^{WT} (SOD1^{WT}-Myc), pcDNA3.1/Myc-SOD1^{G93A} (SOD1^{G93A}-Myc), and pcDNA3.1/Myc-SOD1^{G85R} (SOD1^{G85R}-Myc) were described previously (13, 14). Polyclonal anti-Dorfin (Dorfin-30 and Dorfin-41) and monoclonal anti-VCP antibodies were used as in previous reports (5, 15). The following antibodies were used in this study: monoclonal anti-FLAG antibody (M2; Sigma), monoclonal anti-Myc antibody (9E10; Santa Cruz Biotechnology, Santa Cruz, CA), monoclonal anti-HA antibody (12CA5; Roche Applied Science), polyclonal anti-maltose-binding protein (MBP) antibody (New England BioLabs, Beverly, MA), polyclonal anti-Parkin (Cell Signaling, Beverly, MA), and polyclonal anti-SOD1 (SOD-100; Stressgen, San Diego, CA).

Cell Culture and Transfection—All media and reagents for cell culture were purchased from Invitrogen. HEK293 cells were grown in Dulbecco's modified Eagle's medium containing 10% fetal calf serum, 5 units/ml penicillin, and 50 μg/ml streptomycin. HEK293 cells at subconfluence were transfected with the indicated plasmids using Fu-GENE6 reagent (Roche Applied Science). To inhibit cellular proteasome activity, cells were treated with 1 μM MG132 (benzyloxycarbonyl-Leu-Leu-Leu-al; Sigma) for 16 h after overnight post-transfection. Cells were analyzed at 24–48 h after transfection.

Protein Identification by LC-MS/MS Analysis—FLAG-Dorfin^{WT} was expressed in HEK293 cells (semiconfluent in a 10-cm dish) and then immunoprecipitated by anti-FLAG antibody. The immunoprecipitates were eluted with a FLAG peptide and then digested with Lys-C endopeptidase (*Achromobacter* protease I). The resulting peptides were analyzed using a nanoscale LC-MS/MS system as described previously (16). The peptide mixture was applied to a Mightysil-PR-18 (1-μm particle, Kanto Chemical Corp., Tokyo) column (45 × 0.150 mm ID) and separated using a 0–40% gradient of acetonitrile containing 0.1% formic acid over 30 min at a flow rate of 50 nl/min. Eluted peptides were sprayed directly into a quadrupole time-of-flight hybrid mass spectrometer (Q-Tof *Ultima*; Micromass, Manchester, UK). MS and MS/MS spectra were obtained in data-dependent mode. Up to four precursor ions above an intensity threshold of 10 cps were selected for MS/MS analysis from each survey scan. All MS/MS spectra were searched against protein sequences of Swiss Prot and RefSeq (NCBI) using batch processes of the Mascot software package (Matrix Science, London, UK). The criteria for match acceptance were the following: 1) when the match score was 10 over each threshold, identification was accepted without further consideration; 2) when the difference of score and threshold was lower than 10 or when proteins were identified based on a single matched MS/MS spectrum, we manually confirmed the raw data prior to acceptance; 3) peptides assigned by less than three y series ions and peptides with +4 charge state were all eliminated regardless of their scores.

Recombinant Proteins and Pull-down Assay—We used pMALp2 (New England BioLabs) and pMALp2T (Factor Xa cleavage site of pMALp2 was replaced with a thrombin recognition site) to express fusion proteins with MBP. To produce the full-length (residues 1–838) Dorfin (MBP-Dorfin^{full}), N-terminal (residues 1–367) Dorfin (MBP-Dorfin^N), and C-terminal (residues 368–838) Dorfin (MBP-Dorfin^C), the PCR fragments were amplified from pcDNA4/HisMax-Dorfin (4) by using the appropriate PCR primers with restriction sites (FbaI and HindIII) and then ligated into pMAL-p2 vectors. To produce the MBP-Parkin protein, full-length *PARKIN* cDNA was inserted into the EcoRI-NotI sites of pMALp2T. All of the MBP-tagged recombinant proteins were purified from *Escherichia coli* BL21-codon-plus. The detail of the purification method of MBP-tagged proteins was described previously (17). Recombinant GST fusion VCP^{WT} and VCP^{K524A} proteins were also generated from *E. coli* lysate and purified with glutathione-Sepharose. Recombinant His-VCP^{WT} and His-VCP^{K524A} proteins were purified from insect cells using baculovirus. The detail of purification of these recombinant VCP proteins was described previously (15). Binding experiments were performed with proteins carrying different tags. His- or GST-VCP were mixed with MBP fusion proteins: MBP-Dorfin^{full}, -Dorfin^N, -Dorfin^C, -Parkin, and -mock. His-VCP and GST-VCP proteins were precipitated by Ni^{2+}-nitrilotriacetic acid-agarose (Qiagen, Valencia, CA), and glutathione-Sepharose (Amersham Biosciences), respectively. Binding was performed with 1–3 μg of each protein in 300 μl of binding buffer (50 mM Tris-HCl, pH 7.5, 100 mM NaCl, 5 mM MgCl$_2$, 10% glycerol, 0.5 mg/ml bovine serum albumin, 1 mM dithiothreitol) for 1 h at 4 °C. Then 15 μl of beads were added and incubated for 30 min. The beads were washed by binding buffer three times and eluted with sample buffer and analyzed by SDS-PAGE followed by Western blotting using specific antibodies.

Glycerol Gradient Centrifugation—Cultured cells or mouse tissues were homogenized in 1 ml of PBS with protease inhibitor (Complete Mini; Roche Applied Science). Supernatants (1 mg of protein for cultured cells, 5 mg of protein for mouse tissues, and 0.1 mg of recombinant His-VCP protein) were used as the samples after 10,000 × g centrifugation for 20 min. The samples (1.0 ml) were loaded on top of a 34-ml linear gradient of glycerol (10–40%) prepared in 25 mM Tris-HCl buffer, pH 7.5, containing 1 mM dithiothreitol in 40 PA centrifuge tubes (Hitachi, Tokyo), and centrifuged at 4 °C and 80,000 × g for 22 h using a Himac CP100α centrifuge system (Hitachi). Thirty fractions were collected from the top of the tubes. Two hundred μl of each fraction was precipitated with acetone, and the remaining pellet was lysed with 50 μl of sample buffer and then used for SDS-PAGE followed by Western blotting.

Immunological Analysis—Cells (4 × 10^5 in a 6-cm dish) were lysed with 500 μl of lysis buffer (50 mM Tris-HCl, 150 mM NaCl, 1% Nonidet P-40, and 1 mM EDTA) with protease inhibitor mixture (Complete Mini) 24–48 h after transfection. The lysate was then centrifuged at 10,000 × g for 10 min at 4 °C to remove debris. A 10% volume of the supernatants was used as the "lysate" for SDS-PAGE. When immunoprecipitated, the supernatants were precleared with protein A-Sepharose (Amersham Biosciences), and specific antibodies, anti-FLAG (M2), anti-Myc (9E10), or anti-Dorfin (Dorfin-30) were then added and then incubated at 4 °C with rotation. Immune complexes were then incubated with protein A-Sepharose for 3 h, collected by centrifugation, and washed four times with the lysis buffer. For protein analysis, immune complexes were dissociated by heating in SDS-PAGE sample buffer and loaded onto SDS-PAGE. The samples were separated by SDS-PAGE (12% gel or 4–12% gradient gel) and transferred onto a polyvinylidene difluoride membrane. Finally, Western blotting was performed with specific antibodies.

Immunohistochemistry—HEK293 cells grown on glass coverslips were fixed in 4% paraformaldehyde in PBS for 15 min. Then the cells were blocked for 30 min with 5% (v/v) normal goat serum in PBS, incubated for 1 h at 37 °C with anti-HA antibody (12CA5), washed with PBS, and incubated for 30 min with Alexa 496-nm anti-mouse antibodies (Molecular Probes, Inc., Eugene, OR). The coverslips were washed and mounted on slides. Fluorescence images were obtained using a fluorescence microscope (DMIRE2; Leica, Bannockburn, IL) equipped with a cooled charge-coupled device camera (CTR MIC; Leica). Pictures were taken using Leica Qfluoro software.

Pathological Studies—Pathological studies were carried out on 10% formalin-fixed, paraffin-embedded spinal cords and brain stems filed in the Department of Neurology, Nagoya University Graduate School of Medicine. The specimens were obtained at autopsy from three sporadic cases of ALS and four sporadic PD patients. The spinal cord and brain stem specimens of these ALS and PD cases were immunohistochemically stained with antibodies against Dorfin (Dorfin-41) and VCP. Dou-
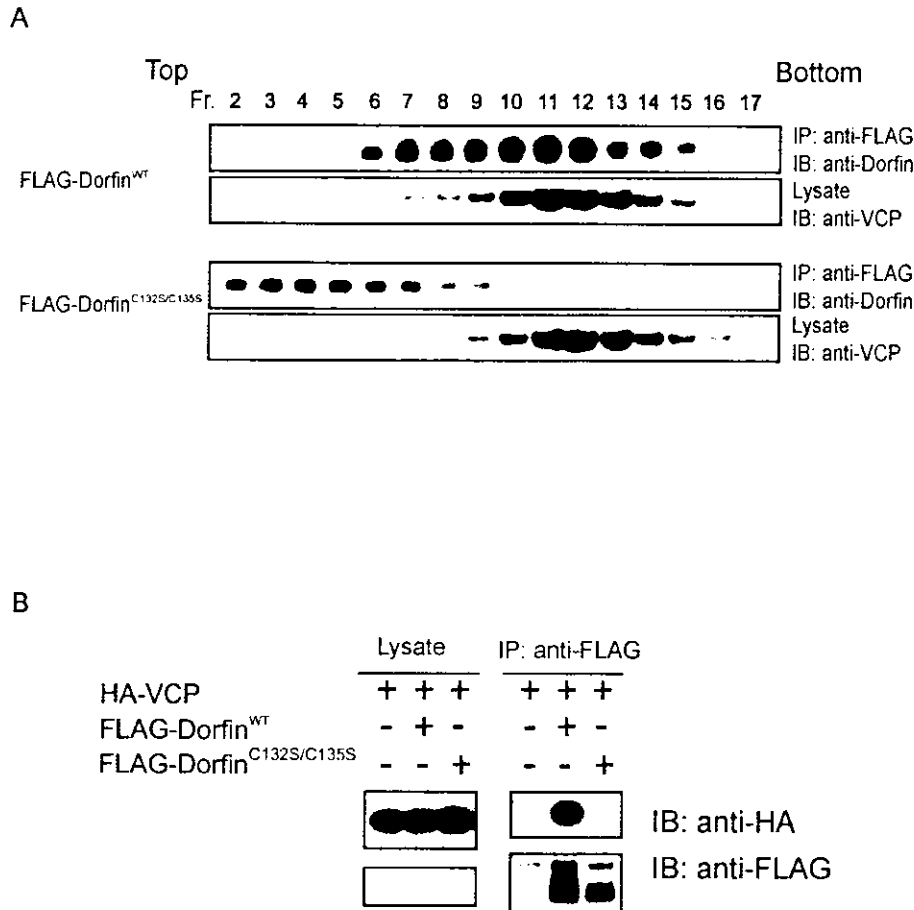
Fig. 1. *In vivo* interaction between Dorfin and VCP. *A*, FLAG-Dorfin and HA-VCP are co-expressed in HEK293 cells. FLAG-mock vector was used as a negative control. The amounts of HA-VCP in 10% of the lysate used are shown (*Lysate*); the rest was subjected to immunoprecipitation (*IP*) with anti-FLAG (M2) antibody. Following immunoblotting (*IB*) with anti-HA (12CA5) antibody revealed that HA-VCP was co-immunoprecipitated with FLAG-Dorfin. *B*, 5 mg of protein of various mouse tissues (brain, liver, kidney, and muscle) and 1 mg of protein of cultured cells (HEK293, HeLa, and Neuro2a) were each homogenized in 1 ml of PBS. Supernatants were fractionated by 10–40% glycerol gradient centrifugation followed by separation into 30 fractions using a fraction collector. Immunoblotting using anti-Dorfin, anti-VCP, and anti-Parkin antibodies was performed on the fractions (*Fr.*), including fractions 2–17. Endogenous Dorfin was co-sedimented with VCP in the fractions with a molecular mass of around 400–600 kDa. The positions of co-migrated molecular mass markers are indicated *above* the *panels*. *C*, immunoprecipitation with polyclonal anti-Dorfin antibody (anti-Dorfin-30) was performed on fractions 11–14 collected by glycerol gradient centrifugation analysis, where endogenous Dorfin was seen in *B*. As a negative control, immunoprecipitation with nonimmune rabbit IgG was used on the same fractions.

ble staining of identical sections was performed as described previously (7). In immunofluorescence microscopy, Alexa-488- and Alexa-546-conjugated secondary antibodies (Molecular Probes) were used. All human and animal studies described in this report were approved by the appropriate Ethics Review Committees of the Nagoya University Graduate School of Medicine.

RESULTS

Identification of Dorfin-associated Protein in the Cells—In an effort to identify protein(s) that physically interacts with Dor-

fin in the cells, FLAG-Dorfin was expressed in HEK293 cells and then immunoprecipitated by anti-FLAG antibody. The immunoprecipitates were eluted with a FLAG peptide and then digested with Lys-C endopeptidase (*Achromobacter* protease I), and the cleaved fragments were directly analyzed using a highly sensitive "direct nanoflow LC-MS/MS" system as described under "Materials and Methods." Following data base search, a total of 13 peptides were assigned to MS/MS spectra obtained from the LC-MS/MS analyses for the FLAG-Dorfin-

A

B

FIG. 2. **Loss of physical interaction between Dorfin$^{C132S/C135S}$ and VCP.** *A*, transfected Dorfin^{WT}, but not Dorfin$^{C132S/C135S}$ (*Dorfin$^{C132S-C135S}$*), forms a high M_r complex. Lysate of HEK293 cells overexpressed with FLAG-Dorfin^{WT} or FLAG-Dorfin$^{C132S/C135S}$ was fractionated by 10–40% glycerol gradient centrifugation. The selected fractions (*Fr.*), fractions 2–17, were subjected to immunoprecipitation (*IP*) using anti-FLAG (M2) antibody. Immunoblotting (*IB*) with anti-Dorfin antibody revealed that exogenous FLAG-Dorfin^{WT} formed a high molecular weight complex, whose peak was at fraction 11, whereas FLAG-Dorfin$^{C132S/C135S}$ migrated in fractions of smaller M_r (around fraction 7). Ten percent of the fractionated samples were shown as "lysate." *B*, Dorfin^{WT} can interact with VCP, but Dorfin$^{C132S/C135S}$ cannot. FLAG-Dorfin^{WT} or FLAG-Dorfin$^{C132S/C135S}$ and HA-VCP were co-expressed in HEK293 cells. FLAG-mock vector was used as a negative control. The amounts of HA-VCP in 10% of the lysate used are shown (*Lysate*); the rest was subjected to immunoprecipitation with anti-FLAG (M2) antibody. Following immunoblotting with anti-HA (12CA5) antibody revealed that HA-VCP was co-immunoprecipitated with FLAG-Dorfin^{WT} but not with FLAG-Dorfin$^{C132S/C135S}$.

associated complexes. These peptide data identified nine proteins as candidates for Dorfin-associated proteins. One of these identified proteins was VCP that has been proposed to have multiple functions, such as membrane fusion or endoplasmic reticulum-associated degradation (ERAD) (18–22). In the next step, we examined the relationship between Dorfin and VCP, because the latter has been reported to be linked to various aspects of neurodegeneration (15).

Dorfin Interacts with VCP in Vivo—To verify the interaction between Dorfin and VCP, FLAG-Dorfin and HA-VCP were transiently overexpressed in HEK 293 cells. Immunological analyses revealed that HA-VCP was co-immunoprecipitated with FLAG-Dorfin but not with FLAG-mock (Fig. 1A), confirming their physical interactions in the cells. To determine whether endogenous Dorfin forms a complex, the lysate from mouse brain homogenate was fractioned by glycerol density gradient centrifugation. Each fraction was immunoblotted with anti-Dorfin antibody. The majority of endogenous Dorfin was co-sedimented with VCP around a size of 400–600 kDa, although endogenous Parkin, which is another RING-IBR type E3 ligase (12), existed in the fractions of much lighter molecular weight (M_r) (Fig. 1B, top panels). Moreover, Dorfin was sedimented in the fractions of 400–600 kDa in other tissues, such as the liver, kidney, and muscle of mouse, and various

cultured cells including Neuro2a, HeLa, and HEK293 cells (Fig. 1B, bottom panels). To determine whether endogenous Dorfin interacts with VCP, immunoprecipitation using polyclonal anti-Dorfin antibody (Dorfin-30) was performed on the fractions shown in Fig. 1B, top panels. Endogenous VCP was co-immunoprecipitated with endogenous Dorfin in the fractions of high M_r (fractions (*Fr.*) 13 and 14). No apparent band was observed when precipitated with rabbit IgG (Fig. 1C).

Mutations of RING Finger Domain of Dorfin Results in Loss of Dorfin-VCP Interactions—Next, we examined whether transfected Dorfin (FLAG-Dorfin^{WT}) and its RING mutant (FLAG-Dorfin$^{C132S/C135S}$), in which the two Cys residues at positions 132 and 135 within the RING finger domain were substituted for Ser residues, form a complex. The results showed overexpression of FLAG-Dorfin^{WT} in high molecular fractions (*Fr.* in Fig. 2), whose peak was between fractions 10 and 12, whereas overexpressed FLAG-Dorfin$^{C132S/C135S}$ did not consist of high molecular weight complex. Overexpression of FLAG-Dorfin^{WT} or FLAG-Dorfin$^{C132S/C135S}$ did not change the sedimentation pattern of VCP (Fig. 2A). Furthermore, immunoprecipitation analysis showed that FLAG-Dorfin^{WT}, but not FLAG-Dorfin$^{C132S/C135S}$, could interact with HA-VCP in HEK293 cells (Fig. 2B).

Dorfin Interacts with VCP in Vitro—To confirm the direct

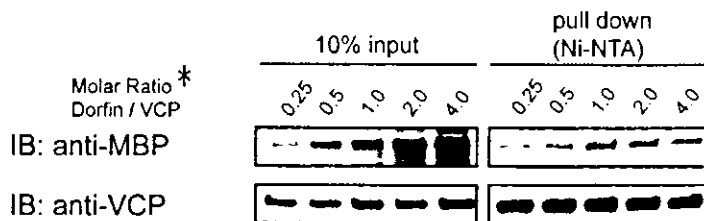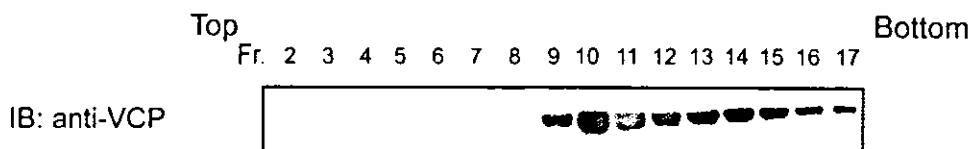*Physical and Functional Interaction between Dorfin and VCP*

A
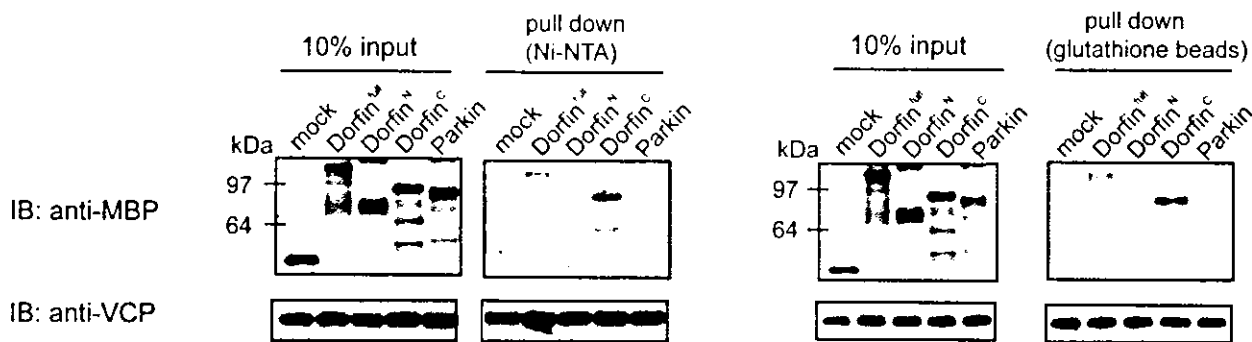
B
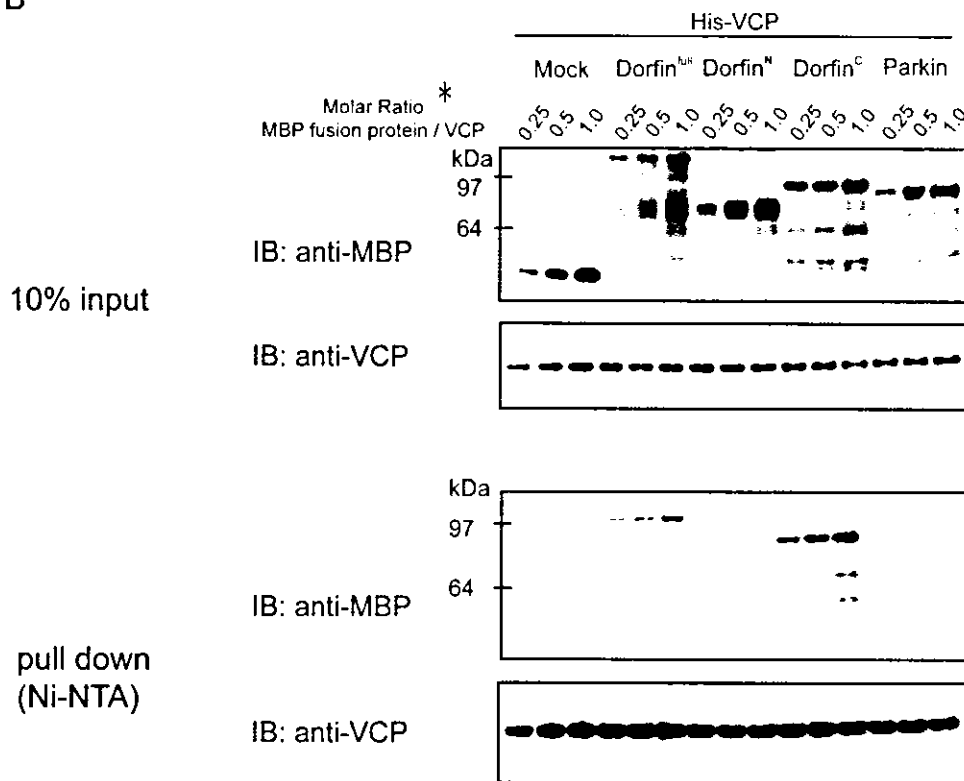
C

D

FIG. 3. *In vitro* interaction between Dorfin and VCP. *A*, recombinant His- or GST-VCP protein was incubated with MBP-mock, MBP-Dorfin^full^, MBP-Dorfin^N^, MBP-Dorfin^C^, and MBP-Parkin proteins *in vitro*. Two µg of His- or GST-VCP proteins and MBP fusion proteins at similar molar concentrations to VCP proteins were used for the assays. The amounts of MBP fusion and GST fusion Dorfin derivatives and His-VCP in 10% of the samples used are shown (*10% input*). *NTA*, nitrilotriacetic acid. *IB*, immunoblot. *B*, 2 µg of His-VCP was incubated with MBP-mock,

binding between Dorfin and VCP and to determine the exact portion of Dorfin that interacts with VCP *in vitro*, we performed pull-down assays using recombinant proteins. Recombinant MBP-Dorfin or its deletion mutants (*i.e.* MBP-Dorfin^N and MBP-Dorfin^C) and the same molar of recombinant His-VCP or GST-VCP were mixed and incubated for 1 h at 4 °C. MBP-mock protein was used as a negative control in these experiments. A small portion of MBP-Dorfin^{full} or Dorfin^C (C-terminal substrate-recognizing domain) bound to both His-VCP and GST-VCP, whereas MBP-mock, MBP-Dorfin^N (N-terminal RING-IBR domain), and MBP-Parkin did not bind to His-VCP or GST-VCP (Fig. 3A). We next determined the number of Dorfins that bind one hexamer of VCP. To investigate this issue, we incubated His-VCP with increasing amounts of MBP-Dorfin^{full}, MBP-Dorfin^N, MBP-Dorfin^C, MBP-mock, or MBP-Parkin. As shown in Fig. 3B, the amount of binding portion of MBP-Dorfin^{full} and -Dorfin^C pulled down with His-VCP was not saturated below the even molar ratio. The pull-down experiments using excess amounts of MBP-Dorfin^{full} revealed that MBP-Dorfin^{full} was saturated at the even molar ratio (Fig. 3C). As reported previously (15), recombinant His-VCP sedimented in high molecular weight fractions, indicating that it formed a hexamer *in vitro* (Fig. 3D). These findings indicated that six Dorfin molecules were likely bind to a VCP complex *in vitro*.

Subcellular Localization of Dorfin and VCP in HEK293 Cells—In previous studies, we showed that exogenous and endogenous Dorfin resided perinuclearly and was colocalized with Vimentin in cultured cells treated with a proteasome inhibitor (4). The staining patterns of Dorfin were indistinguishable from those of the aggresome, namely a pericentriolar, membrane-free, cytoplasmic inclusion containing misfolded ubiquitylated proteins packed in a cage of intermediate filaments (4). VCP immunostaining was also observed throughout aggresomes in cultured neuronal cells when induced by treatment with a proteasome inhibitor (15). In order to examine the subcellular localization of Dorfin and VCP, GFP-Dorfin and HA-VCP were co-expressed in HEK293 cells. Without proteasome treatment, GFP-Dorfin-expressing cells showed granular fluorescence in the cytosol, and the HA-VCP-expressing cells showed diffuse and uniform cytoplasmic staining (Fig. 4A). Treatment with MG132 (1 μM, 16 h) resulted in accumulation of both GFP-Dorfin and HA-VCP and perinuclear colocalization as a clear large protein aggregate that mimics aggresomes (Fig. 4B).

Colocalization of Dorfin and VCP in the Affected Neurons of ALS and PD—In previous studies, immunostaining of Dorfin and VCP was independently noted in LBs of PD, and the peripheral staining pattern of both proteins in LBs was similar (7, 23). To confirm the immunoreactivities of Dorfin and VCP in the affected neurons in ALS and PD, we performed a double-labeling immunofluorescence study using a rabbit polyclonal anti-Dorfin antibody (Dorfin-41) and a mouse monoclonal VCP antibody on the postmortem samples of ALS and PD. In the ALS spinal cords, both proteins were colocalized in the LB-like inclusions (Fig. 5, A–F). The margin of LBs in PD was intensely immunostained for Dorfin and VCP, and merged images confirmed their strong colocalization (Fig. 5, G–L). Dorfin and VCP were also positive in Lewy neurites in the affected neurons of PD (Fig. 5, M–O).
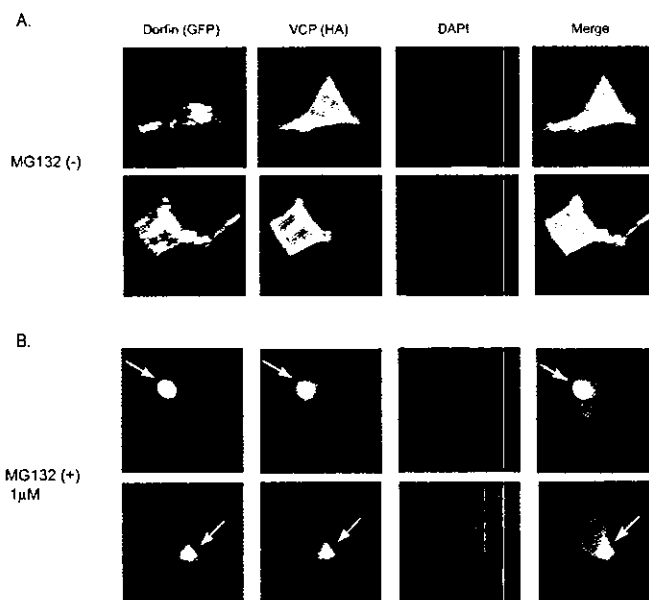

A.

Dorfin (GFP) VCP (HA) DAPI Merge

MG132 (-)

B.

MG132 (+)
1μM

Fig. 4. **Subcellular localization of GFP-Dorfin and HA-VCP in HEK293 cells treated or untreated with a proteasome inhibitor.** GFP-Dorfin and HA-VCP were co-expressed transiently in HEK 293 cells. Cells were treated with (*B*) or without (*A*) 1 μM MG132 for 16 h. HA-VCP was stained with anti-monoclonal HA antibody (12CA5). Nuclei were stained with 4',6-diamidino-2-phenylindole (*DAPI*). Without the treatment of MG132, GFP-Dorfin was spread through the cytosol, and it appeared like small aggregations. HA-VCP was also seen mainly in the cytosol and partly colocalized with GFP-Dorfin (*A*). After treatment with 1 μM MG132 for 16 h, both GFP-Dorfin and HA-VCP showed perinuclear accumulation and colocalization and appeared as clear large protein aggregates (*B*; *arrows*).

Dorfin Ubiquitylates Mutant SOD1 in Vivo—Unlike the wild-type form, mutant SOD1 proteins are rapidly degraded by the ubiquitin-proteasome system. Consistent with our previous results (5), SOD1^{G93A} and SOD1^{G85R} were polyubiquitylated, and co-expression with FLAG-Dorfin^{WT} enhanced polyubiquitylation of these mutant SOD1s compared with co-expression with FLAG-BAP, a negative control construct (Fig. 6A). Boiling with 1% SDS-containing buffer did not change the level of ubiquitylated mutant SOD1, indicating that mutant SOD1 itself was ubiquitylated by Dorfin (Fig. 6B). We also performed the same *in vivo* ubiquitylation assay using Neuro2a cells to examine for E3 activity of Dorfin in neuronal cells. The enhanced polyubiquitylation of these mutant SOD1s by Dorfin was observed in Neuro2a cells as well as in HEK293 cells (Fig. 6C). FLAG-Dorfin$^{C132S/C135S}$ did not enhance polyubiquitylation of mutant SOD1s, indicating that this RING finger mutant form was functionally inactive (Fig. 6D).

VCP^{K524A} Suppresses the E3 Activity of Dorfin—VCP has two ATPase binding domains (D1 and D2). A D2 domain mutant, VCP^{K524A}, induces cytoplasmic vacuoles, which mimics vacuole formation seen in the affected neurons in various neurodegenerative diseases (11, 15). The D2 domain represents the major ATPase activity and is essential for VCP function (11). The ATPase activity of VCP^{K524A} is much lower than that of VCP^{WT}, and VCP^{K524A} caused accumulation of polyubiquitylated proteins in the nuclear and membrane fractions together with elevation of ER stress marker proteins due to ERAD

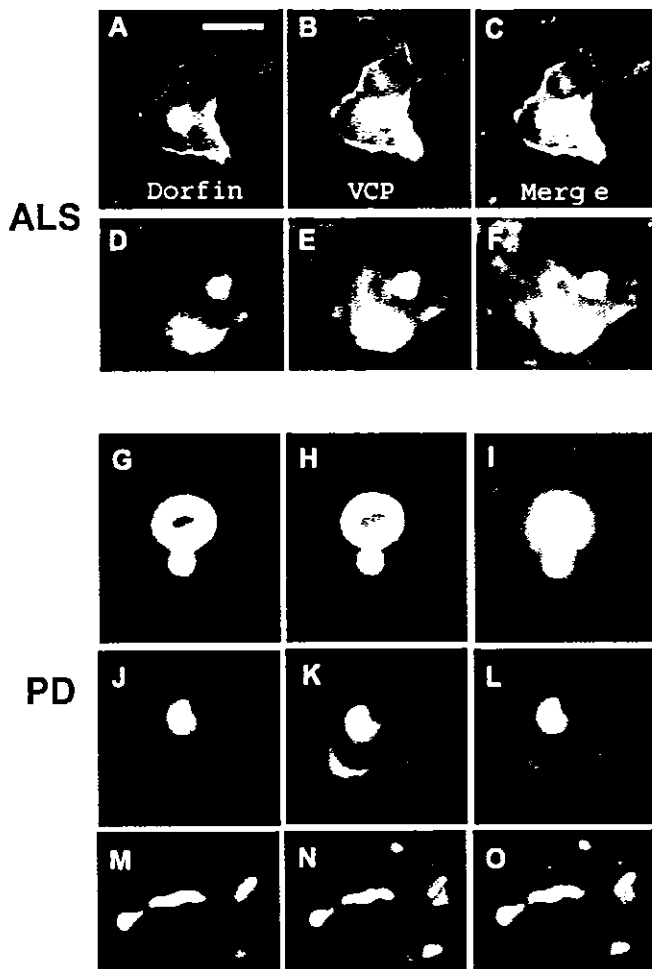*Physical and Functional Interaction between Dorfin and VCP*

FIG. 5. **Colocalization of Dorfin-41 immunoreactivity with VCP in neuronal inclusions in ALS and PD.** Sections were doubly labeled with anti-Dorfin-41 antiserum and monoclonal VCP antibody and analyzed with a laser-scanning confocal microscope. The *left panels* (*green*) correspond to Dorfin, *middle panels* (*red*) correspond to VCP, and *right panels* correspond to merged images; structures in *yellow* indicate colocalization. Colocalization of Dorfin and VCP is seen in LB-like inclusions in motor neurons of the spinal cord of ALS (*A–F*). Dorfin is also colocalized with VCP in the margin of LBs (*G–I*), premature LBs (*J–L*), and Lewy neurites (*M–O*) in the nigral neurons of PD. *Scale bars*, 20 μm (*A–L*) and 10 μm (*M–O*).

inhibition, whereas its expression level, localization, and complex formation were indistinguishable from those of VCP^{WT} (11). In order to examine the functional effect of VCP on Dorfin, VCP^{WT}, VCP^{K524A}, or LacZ was co-expressed with SOD1^{G85R}, FLAG-Dorfin, and HA-Ub in HEK293 cells. Co-expression with VCP^{K524A} showed a marked decline of polyubiquitylation of SOD1^{G85R} compared with co-expression with VCP^{WT} or LacZ (Fig. 7A, *top* and *middle*). Since Dorfin physically interacts with mutant SOD1s (5), we next investigated whether this decline of polyubiquitylation of SOD1^{G85R} was mediated by reduced affinity between SOD1^{G85R} and Dorfin. Immunoprecipitation by anti-FLAG antibody showed that VCP^{K524A} did not change affinity between SOD1^{G85R} and Dorfin (Fig. 7A, *bottom*). Neither VCP^{WT} nor VCP^{K524A} changed the level of polyubiquitylation protein in the total lysate (Fig. 7B). To clarify whether this negative effect of VCP^{K524A} is specific for Dorfin, we assessed the autoubiquitylation of FLAG-Parkin in the presence of VCP^{WT}, VCP^{K524A}, or LacZ. Co-expression of VCP^{K524A} did not decrease autoubiquitylation of FLAG-Parkin compared with co-expression of LacZ or VCP^{WT} (Fig. 7C). We performed the same experiments using Neuro2a cells to see whether VCP^{K524A} suppress the E3 activity of Dorfin in neu-

ronal cells. The marked decline of polyubiquitylation of SOD1^{G85R} by VCP^{K524A} expression was also seen in Neuro2a cells (Fig. 7D).

DISCUSSION

UBIs in the affected neurons are histopathological hallmarks in various neurodegenerative disorders (8). Dorfin is an E3 ligase, which can ubiquitylate mutant SOD1s and synphilin-1 (5, 24). These substrates and Dorfin were identified in UBIs in various neurodegenerative diseases, such as LB-like inclusions in ALS and LBs in PD and dementia with Lewy bodies (7). This finding suggests that Dorfin may play a crucial role in the process of generating inclusions in the affected neurons. In the present study, we identified VCP as one of the Dorfin-associated proteins using mass spectrometry, and VCP-Dorfin physical interaction was confirmed by an immunoprecipitation experiment using FLAG-Dorfin and HA-VCP overexpressed in HEK293 cells (Fig. 1A). VCP is an essential and highly conserved protein of the AAA-ATPase family, which is considered to have diverse cellular functions, such as membrane fusion (25–27), nuclear trafficking (28), cell proliferation (29, 30), and the ERAD pathway (18–22). Many reports have implied that VCP is involved in the pathogenesis of various neuromuscular diseases. VCP has been implicated as a factor that modifies the progress of polyglutamine-induced neuronal cell death (15). In addition, histopathological studies revealed positive staining for VCP in UBIs in PD and ALS with dementia (23). VCP is also associated with MJD protein/atxin-3, in which abnormal expansion of polyglutamine tracts causes Machado-Joseph disease/spinocerebellar ataxia type 3 (31). VCP is also required for the degradation of ataxin-3 in collaboration with E4B/Ufd2a, a ubiquitin chain assembly factor (E4) (32). Recent studies have indicated that missense mutations in the VCP gene cause inclusion body myopathy associated with Paget's disease of bone and frontotemporal dementia, which is characterized by the presence of vacuoles in the cytoplasm in muscle fibers (33).

Our results showed that endogenous Dorfin formed a 400–600-kDa complex in various tissues and various cultured cells (Fig. 1B). Dorfin is a ~91-kDa protein; therefore, this high M_r complex should include Dorfin-associated proteins, although the possibility that Dorfin itself oligomerizes in the cell cannot be excluded. Glycerol gradient centrifugation analysis and immunoprecipitation experiments in the present study showed that endogenous Dorfin interacted with endogenous VCP in a complex of approximately 600 kDa, possibly including a Dorfin molecule and a hexametric form of VCP (Fig. 1C).

The first RING mutant of Dorfin, in which Cys at positions 132 and 135 changed to Ser, was prepared. This mutant Dorfin, Dorfin$^{C132S/C135S}$, could not ubiquitylate mutant SOD1s (Fig. 6D). Glycerol gradient centrifugation analysis revealed that Dorfin$^{C132S/C135S}$ did not form a high M_r complex, whereas exogenous wild type Dorfin (Dorfin^{WT}) formed a high M_r complex similar to endogenous Dorfin (Fig. 2A). Furthermore, an immunoprecipitation experiment using Dorfin^{WT} and Dorfin$^{C132S/C135S}$ revealed that Dorfin^{WT} could interact with VCP, whereas Dorfin$^{C132S/C135S}$ could not (Fig. 2B).

Our *in vitro* study using recombinant proteins showed that full-length (MBP-Dorfin^{full}) and the C terminus of Dorfin (MBP-Dorfin^{C}) directly interacted with VCP, whereas the MBP-Dorfin^{N} mutant, containing the entire RING finger domain (amino acid residues 1–367), did not bind to VCP (Fig. 3A). This finding was unexpected, since *in vivo* binding analysis suggested that Dorfin could interact with VCP at the RING finger domain. It is plausible that certain structural changes in Dorfin$^{C132S/C135S}$ might render the C-terminal VCP-binding portion incapable of accessing VCP molecules. This may explain the result that Dorfin$^{C132S/C135S}$ did not form a high M_r complex.
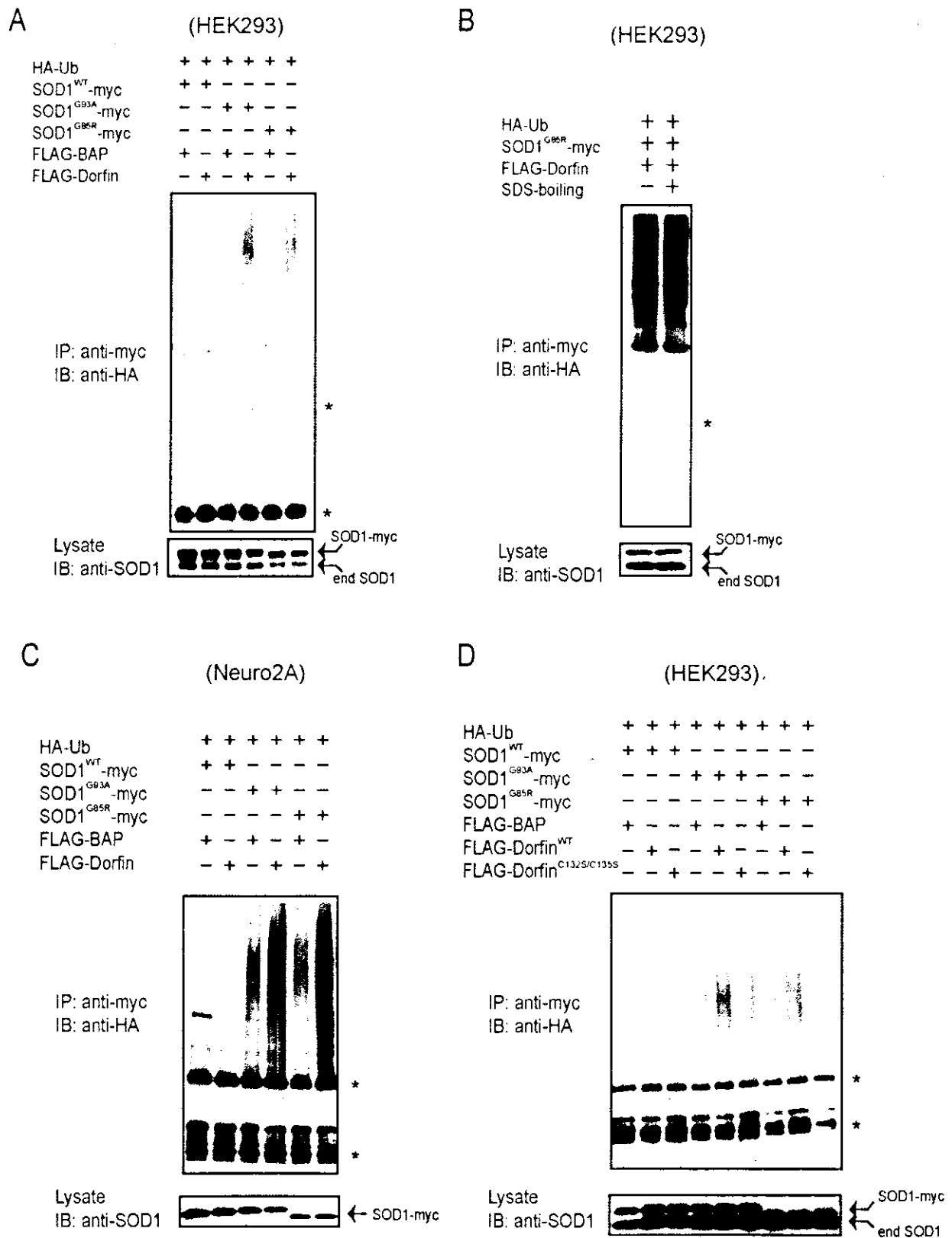
FIG. 6. **Dorfin ubiquitylates mutant SOD1s *in vivo*.** *A*, increased ubiquitylation of mutant SOD1 proteins by overexpression of Dorfin. HEK293 cells were co-transfected with SOD1^{WT}-Myc, SOD1^{G93A}-Myc, or SOD1^{G85R}-Myc and HA-Ub with or without FLAG-Dorfin. FLAG-bovine alkaline phosphatase (*BAP*) was used as a negative control. Immunoprecipitation (*IP*) was performed with Myc antibody (9E10). *IB*, immunoblotting. *B*, SDS boiling was performed prior to immunoprecipitation. To examine covalently ubiquitylated molecules, the cell lysate was boiled with the buffer containing 1% SDS for 5 min. Immunoprecipitation with Myc antibody (9E10) showed that the SDS-boiling procedure did not change polyubiquitylation level of SOD1^{G85R}-Myc by Dorfin. *C*, increased ubiquitylation of mutant SOD1 proteins by overexpression of Dorfin in Neuro2a cells. The same *in vivo* ubiquitylation assay as in *A* was performed using Neuro2a cells. *D*, Dorfin$^{C132S/C135S}$ (Dorfin$^{C132S/C135S}$) did not have E3 activity on mutant SOD1. HEK293 cells were co-transfected with SOD1^{WT}-Myc, SOD1^{G93A}-Myc, or SOD1^{G85R}-Myc and HA-Ub with FLAG-Dorfin^{WT} or FLAG-Dorfin$^{C132S/C135S}$. The *asterisks* indicate IgG light and heavy chains.

A

(HEK293)

HA-Ub	+	+	+
SOD1^{G85R}-myc	+	+	+
FLAG-Dorfin	+	+	+
LacZ	+	−	−
VCP^{WT}	−	+	−
VCP^{K524A}	−	−	+

IP: anti-myc
IB: anti-HA

*
*

Lysate
IB:anti-SOD1
SOD1-myc
end SOD1

IP: anti-FLAG
IB: anti-SOD1
← SOD1-myc

B

(HEK293)

HA-Ub	+	+	+
SOD1^{G85R}-myc	+	+	+
FLAG-Dorfin	+	+	+
LacZ	+	−	−
VCP^{WT}	−	+	−
VCP^{K524A}	−	−	+

Lysate
IB:anti-HA

C

(HEK293)

HA-Ub	+	+	+
FLAG-Parkin	+	+	+
LacZ	+	−	−
VCP^{WT}	−	+	−
VCP^{K524A}	−	−	+

IP: anti-FLAG
IB: anti-HA

*
*

Lysate
IB: anti-Parkin

D

(Neuro2A)

HA-Ub	+	+	+
SOD1^{G85R}-myc	+	+	+
FLAG-Dorfin	+	+	+
LacZ	+	−	−
VCP^{WT}	−	+	−
VCP^{K524A}	−	−	+

IP: anti-myc
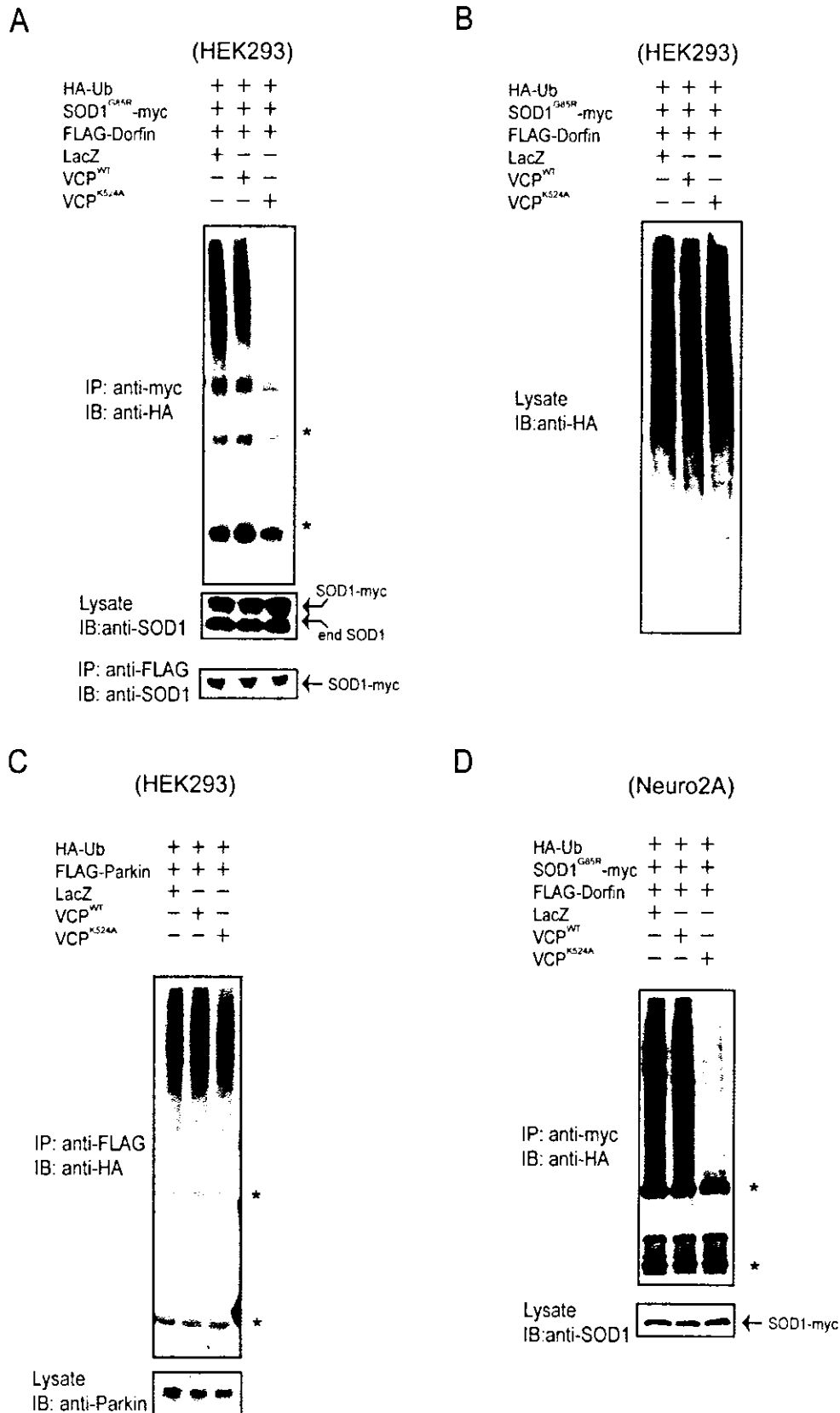IB: anti-HA

*
*

Lysate
IB:anti-SOD1
← SOD1-myc

FIG. 7. **A dominant negative mutant of VCP, VCP^{K524A} inhibits the E3 ubiquitin ligase activity of Dorfin.** *A*, inhibition of dominant negative form mutant VCP^{K524A} on the E3 ubiquitin ligase activity of Dorfin. HEK293 cells were co-transfected with SOD1^{G85R}-Myc, HA-Ub, FLAG-Dorfin, and VCP^{WT}, VCP^{K524A}, or LacZ. Immunoprecipitation (*IP*) was performed with Myc antibody (9E10) and FLAG antibody (M2). *IB*, immunoblotting. *B*, neither VCP^{WT} nor VCP^{K524A} changed the level of total polyubiquitylated protein in the cell lysate. Ten percent of the volume of HEK293 cells used in *A* was subjected to immunoblotting using anti-HA (12CA5) antibody. *C*, autoubiquitylation of FLAG-Parkin was not influenced by the dominant negative form VCP^{K524A}. HEK293 cells were co-transfected with FLAG-Parkin, HA-Ub, and VCP^{WT}, VCP^{K524A}, or LacZ. Immunoprecipitation with FLAG antibody (M2) was performed. *D*, inhibition of VCP^{K524A} on E3 ubiquitin ligase activity of Dorfin in Neuro2a cells. Neuro2a cells were co-transfected with SOD1^{G85R}-Myc, HA-Ub, FLAG-Dorfin, and VCP^{WT}, VCP^{K524A}, or LacZ. Immunoprecipitation was performed using Myc antibody (9E10) and FLAG antibody (M2). The *asterisks* indicate IgG light and heavy chains.